Journal of Medicinal Chemistry



Article

# Discovery of Potent, Selective and Peripherally Restricted Pan-Trk Kinase Inhibitors for the Treatment of Pain

Sharan K Bagal, Mark Andrews, Bruce M. Bechle, Jianwei Bian, James Bilsland, David C Blakemore, John Braganza, Peter J. Bungay, Matthew S. Corbett, Ciarán N Cronin, Jingrong Jean Cui, Rebecca Dias, Neil J Flanagan, Samantha E Greasley, Rachel Grimley, Kim James, Eric Johnson, Linda Kitching, Michelle L Kraus, Indrawan McAlpine, Asako Nagata, Sacha Ninkovic, Kiyoyuki Omoto, Stephanie Scales, Sarah E. Skerratt, Jianmin Sun, Michelle Tran-Dubé, Gareth J. Waldron, Fen Wang, and Joseph S Warmus

*J. Med. Chem.*, **Just Accepted Manuscript** • DOI: 10.1021/acs.jmedchem.8b00633 • Publication Date (Web): 26 Jun 2018

# Discovery of Potent, Selective and Peripherally Restricted Pan-Trk Kinase Inhibitors for the Treatment of Pain

*Sharan K. Bagal,[a*] Mark Andrews,[d] Bruce M. Bechle [e] Jianwei Bian, [e] James Bilsland,[c] David C. Blakemore,[a] John F. Braganza, [f] Peter J. Bungay,[b] Matthew S. Corbett, [e] Ciaran N. Cronin,[f] Jingrong Jean Cui,[f] Rebecca Dias,[c] Neil J. Flanagan,[c] Samantha E. Greasley,[f] Rachel Grimley,[c] Kim James,[g] Eric Johnson,[f] Linda Kitching,[c] Michelle L. Kraus,[f] Indrawan McAlpine,[f] Asako Nagata,[f] Sacha Ninkovic, [f] Kiyoyuki Omoto,[a] Stephanie Scales [f], Sarah E. Skerratt,[a] Jianmin Sun,[e] Michelle Tran-Dubé, [f] Gareth J. Waldron,[c] Fen Wang, [f] Joseph S. Warmus.[e]*

[a]Worldwide Medicinal Chemistry, Pfizer Worldwide R&D UK, The Portway Building, Granta Park, Cambridge, CB21 6GS, UK

[b]Pharmacokinetics, Dynamics & Metabolism, Pfizer Worldwide R&D UK, The Portway Building, Granta Park, Cambridge CB21 6GS, UK

[c]Pfizer Worldwide R&D UK, The Portway Building, Granta Park, Cambridge CB21 6GS, UK

[d]Pfizer Worldwide R&D UK, Sandwich, Kent, CT13 9NJ, UK

[e]Pfizer Worldwide R&D, Groton Laboratories, Eastern Point Road, Groton, Connecticut 06340, USA

[f]Pfizer Worldwide R&D, La Jolla Laboratories, 10770 Science Center Drive, San Diego, California, 92121, USA

[g]Peakdale Molecular, Discovery Park House, Ramsgate Road, Sandwich CT13 9ND, UK

**KEYWORDS**

Nerve growth factor receptor, NTRK1, NTRK2, NTRK3, NGF, TrkA, TrkB, TrkC, pan-Trk, Tropomyosin Receptor Kinase, Kinase inhibitor

## ABSTRACT

Hormones of the neurotrophin family: nerve growth factor (NGF), brain derived neurotrophic factor (BDNF), neurotrophin 3 (NT3) and neurotrophin 4 (NT4) are known to activate the family of Tropomyosin receptor kinases (TrkA, TrkB, TrkC). Moreover, inhibition of the TrkA kinase pathway in pain has been clinically validated by the NGF antibody tanezumab leading to significant interest in the development of small molecule inhibitors of TrkA. Furthermore, Trk inhibitors having an acceptable safety profile will require minimal brain availability. Herein we discuss the discovery of two potent, selective, peripherally restricted, efficacious and well-tolerated series of pan-Trk inhibitors which successfully delivered three candidate quality compounds **10b, 13b** and **19**. All three compounds are predicted to possess low metabolic clearance in human that does not proceed via aldehyde oxidase-catalyzed reactions, thus addressing the potential clearance prediction liability associated with our current pan-Trk development candidate PF-06273340.

## INTRODUCTION

Hormones of the neurotrophin family: nerve growth factor (NGF), brain derived neurotrophic factor (BDNF), neurotrophin 3 (NT3) and neurotrophin 4 (NT4) are known to activate the family of Tropomyosin receptor kinases (TrkA, TrkB, TrkC).[1] In particular, NGF has been shown to have a key role in the pathogenesis of inflammatory pain in preclinical studies.[2] Moreover, clinical studies in osteoarthritis, chronic low back pain and interstitial cystitis have demonstrated that NGF neutralizing antibodies such as tanezumab demonstrate robust efficacy. [3 4 5 6] Since the NGF pathway involves NGF binding to the TrkA kinase receptor, inhibition of TrkA has been clinically validated as a target for pain leading to increased interest in the development of small molecule inhibitors of TrkA.

The majority of small molecule kinase inhibitors tend to be ATP competitive Type I or Type II binders, based on the conformation of the highly conserved aspartate-phenylalanine-glycine (DFG) residues in the beginning of the activation loop in the kinase domain.[7-8] Type I and Type II binders of TrkA tend to exhibit pan-Trk (TrkA/B/C) inhibition rather than subtype selectivity because TrkA, TrkB and TrkC kinases have no residue differences in the ATP binding site.[9] Furthermore, Pan-Trk inhibitors require restriction to the peripheral compartment to avoid undesirable side effects associated with Trk inhibition in the central nervous system (CNS). TrkA is highly expressed in cholinergic neurons of the CNS with ablation of the TrkA gene in preclinical species leading to dysfunction in cholinergic circuitry.[10-12] TrkB is expressed throughout the body and is involved in excitatory signaling, long-term potentiation and feeding behavior.[13,14,15-16] Moreover, human genetic data has associated TrkB with obesity and development.[17] TrkC is widely expressed in neural and non-neural tissues and plays a role in the development and survival of the sympathetic nervous system.[18-19] Finally, clinical studies on the CNS penetrant pan-Trk/Tie2

kinase inhibitor CE-245677 (advanced by Pfizer as an oncology agent), produced CNS side-effects leading to the termination of Phase I multiple dose trials. The reported adverse events fully resolved upon cessation of dosing and included cognitive problems, personality changes and sleep disturbances.[20] Given that the safety and toleration risks are associated with CNS Trk receptor occupancy and efficacy of Trk kinase inhibitors is expected to be driven by target engagement in peripheral neurons we can address the safety risks by restricting Trk inhibitors to the peripheral compartment. This profile would require small molecule TrkA inhibitors that possess acceptable oral bioavailability but which are also peripherally restricted.[21-25] These properties can be designed by operating within physicochemical space appropriate for absorption across the gastrointestinal (GI) epithelium (e.g. molecular weight (MW) <500, polar surface area (PSA) <140, <10 rotatable bonds),[26] whilst combining activity as substrates for the efflux transporters P-glycoprotein (P-gp) and Breast Cancer Resistance Protein (BCRP) that are expressed at the blood-brain barrier (BBB).[21-23, 27] However, targeting P-gp and BCRP, which are also present in the apical membrane of intestinal epithelial cells, introduces the risk of restricting transport across the intestinal epithelium, resulting in low and variable oral bioavailability. This risk, however, is low because adequately soluble oral drugs at commonly prescribed doses are expected to saturate efflux transporters, given that substrates of P-gp typically possess Km values in the range 1−100 μM. In addition, the high concentration gradient across the intestinal epithelium will lead to a significant driving force for flux of compound, particularly for drugs with high intrinsic permeability.[28]

We have previously reported the discovery of our pan-Trk development candidate PF-06273340 (Figure 1).[9, 29] The profile of metabolism of this compound involved a component that was mediated by aldehyde oxidase (AO) reducing the confidence with which human metabolic clearance (CL) could be predicted.[30] Hence, contingency pan-Trk candidates were sought,

whereby AO-mediated metabolism was avoided in order to mitigate human pharmacokinetic (PK) risk associated with PF-06273340. This work describes the discovery of three candidate quality pan-Trk compounds that have high confidence in human PK prediction.

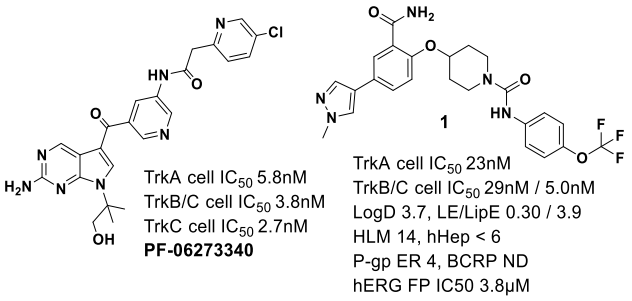


**Figure 1.** Pfizer Pan-Trk development candidate PF-06273340 and hit molecule **1**

## RESULTS AND DISCUSSION

**Hit identification and optimization.** In order to find novel pan-Trk chemical matter the Pfizer kinase selectivity dataset was analyzed. This dataset is a collection of compounds that have been assessed for off target kinase selectivity at Invitrogen by screening in a kinase selectivity panel. The Pfizer kinase selectivity panel included a TrkA assay in a Z'-LYTE biochemical assay format, whereby benzamide hit **1** was identified as having 98% inhibition of TrkA at 1μM (Figure 1). Furthermore, **1** was found to be a potent pan-Trk inhibitor in cell based assays with TrkA cell $IC_{50}$ 23nM and TrkB/C cell $IC_{50}$ <30nM.[31] Benzamide hit **1** exhibited a ligand efficiency (LE) 0.3 and lipophilic efficiency (LipE) 3.9 (LipE= -Log(TrkA cell $IC_{50}$)- LogD) both of which were considered acceptable start points for optimization. Moreover, **1** had low metabolic turnover in

human liver microsomes (HLM) and human hepatocytes (hHep) (intrinsic clearance ($CL_{int}$) in HLM 14μL/min/mg protein, hHep <6μL/min/million cells) suggesting that this benzamide series was capable of delivering compounds with low predicted human CL. In order to achieve restriction from the CNS to the periphery and avoid unwanted CNS side effects P-gp and BCRP efflux transporter substrates are required. P-gp and BCRP substrates are determined as having an efflux ratio (ER) >2.5 in the current assay format to assess P-gp and BCRP efflux. Hit molecule **1** was a P-gp substrate with an efflux ratio (ER) of 4 (BCRP not determined) indicating this benzamide series had potential for the desired restriction to the peripheral compartment. The combination of potency, LE, LipE, metabolic stability and P-gp efflux suggested that **1** was an exciting hit that warranted further investment.

The human Ether-à-go-go-Related Gene (hERG) fluorescence polarization (FP) competition assay and patch express assay (PX) have been shown to be predictive of compound QT prolongation effects via hERG blockade.[32] The hERG FP assay can also be run in a high throughput 384-well plate manner.[32] Hit molecule **1** was shown to inhibit hERG in the hERG FP assay (hERG FP $IC_{50}$ 3.8μM) indicating there was some cardiovascular risk, which may have been associated with the relatively high LogD of **1** (LogD 3.7).[33] Modification of urea **1** to an amide **2** improved potency and lowered LogD moderately (TrkA cell $IC_{50}$ 8.7nM, LogD 3.5) such that LipE improved by 0.7 units to 4.6, although hERG FP $IC_{50}$ did not improve significantly (Figure 2). Additional improvements in LipE were made by changing the N-methyl pyrazole into the isomeric N-methyl imidazole **3** (LipE 5.3) through decreasing LogD further (LogD 2.9) whilst maintaining potency (Figure 2). Furthermore, the reduction in LogD led to a concomitant decline in hERG liability (hERG FP $IC_{50}$ 18μM). Ligand **3** was also assessed in the hERG PX assay which suggested **3** was >1300-fold selective for TrkA in cell based assays over hERG inhibition (TrkA cell $IC_{50}$ 7.0nM,

hERG PX $IC_{50}$ 9500nM), making it an excellent lead molecule. Ligand **3** exhibited low turnover in HLM and hHep ($CL_{int}$ HLM <8 μL/min/mg protein; hHep 8 μL/min/million cells). Moreover, metabolite identification studies suggested the major metabolism pathways involved only phase I oxidative pathways catalyzed by cytochrome P450 (CYP) (data not shown). Thus, the absence in **3** of metabolism catalyzed by AO, would lend higher confidence to predictions made from in vitro metabolic CL when compared with PF-06273340 (Figure 1). The passive permeability of **3** was measured in the RRCK transcellular flux assay (RRCK $P_{app}10x10^{-6}cms^{-1}$) and was consistent with good absorption.[31, 34-35]

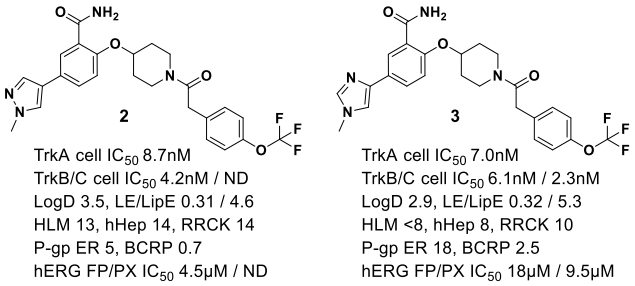


**Figure 2.** Discovery of benzamide lead molecule **3**

Lead molecule **3** was progressed to oral and i.v. pharmacokinetic (PK) studies in rats and demonstrated moderate systemic CL (plasma CL 38 mL/min/Kg), and moderate oral bioavailability (45%), consistent with complete absorption. The ability of **3** to act as a substrate for P-gp and BCRP was also assessed and **3** was found to be a substrate for both these transporters (P-gp ER 18, BCRP ER 2.5). Ligand **3** was progressed to CNS penetration studies in rat in order to understand the level of restriction from the CNS achievable, and was found to be peripherally restricted with $C_{b,u}/C_{p,u}$ of 0.0065. These data provided evidence that restriction from the CNS combined with acceptable oral absorption was indeed achievable in this chemical series. The

binding mode of **3** was determined via X-ray crystallography with a 2.91Å co-crystal structure of **3** with TrkA protein (Figure 3). Ligand **3** was a Type II inhibitor which binds to the DFG-out conformation of TrkA formed by the movement of the activation loop to an inactive conformation. The movement of the activation loop involves relocation of the DFG motif which creates an unoccupied back pocket.[7-8] In the case of ligand **3** the back pocket is occupied by the p-$OCF_3$ aryl group. The primary carboxamide of **3** interacts with the kinase hinge through hydrogen bonds between the ligand C=O and backbone NH of Met592, and ligand NH with the backbone C=O of Glu590. Ligand **3** extends into TrkA passing the gatekeeper Phe589 and DFG Phe669 and these phenylalanine residues sandwich the piperidine linker, with the central amide carbonyl of **3** forming a hydrogen bond with the backbone NH of Asp668. The p-$OCF_3$ aryl group occupied the back pocket and there was a CH-π interaction between this aryl unit and the backbone CH of Gly667. The N-methyl imidazole had a vector towards the solvent exposed kinase exit which suggested that the structure activity relationship (SAR) in this region will be relatively tolerant, which for example, explained the similar TrkA cellular potencies of inhibitors **2** and **3** (Figure 2). Variation of the p-$OCF_3$ aryl group revealed a number of potential replacements although since the back pocket was formed by hydrophobic residues such as Leu564, Leu567, Phe646, Ile666 the active back pocket substituents identified were relatively lipophilic (Table 1). Substitution of the benzylic carbon was tolerated by TrkA as exemplified by **4** and **5** although one enantiomer was over 60-fold more potent than the other (TrkA cell $IC_{50}$ **4:** 0.011μM and **5:** 0.72μM), presumably due to a clash between the benzylic methyl substituent and Phe589 in **5**. Substitution of the p-$OCF_3$ aryl group by 3-F in **6** was tolerated by TrkA but did not offer any advantages when compared with the unsubstituted analogue **3**. The p-$OCF_3$ substituent was successfully replaced by a cyclopropyl ether as demonstrated by ligand **7** and this modification improved hERG liability

considerably (hERG FP $IC_{50}$ > 40μM). However, the cyclopropyl ether unit underwent greater metabolic CL in HLM (HLM 23μL/min/mg protein) when compared with lead molecule **3** (HLM <8μL/min/mg protein). At this stage in the program the p-$OCF_3$ phenyl group in **3** was favored as a back pocket substituent based on TrkA cell potency, LipE and metabolic CL. The benzamide in **3** could be successfully replaced by a nicotinamide as demonstrated by **8** (Table 1). Nicotinamide **8** exhibited a similar TrkA potency to **3** but had a lower LogD (**8:** LogD 2.4, **3:** LogD 2.9) and hence a greater LipE than **3**.[31]

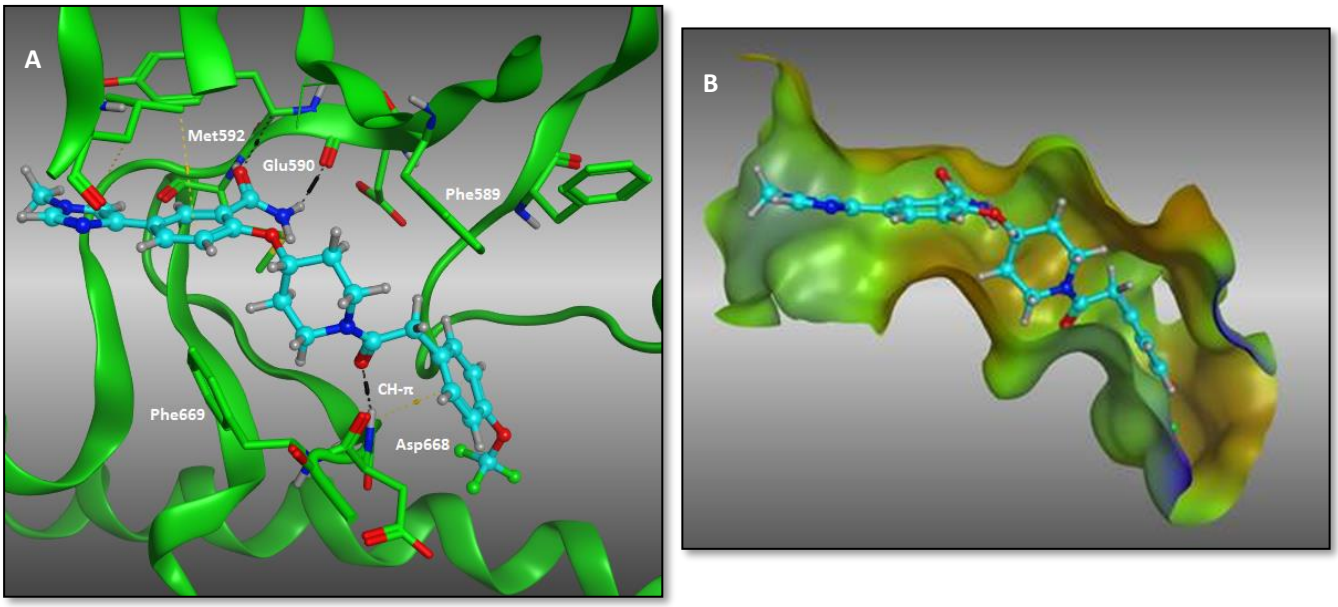


**Figure 3.** A) Co-crystal structure of lead molecule **3** bound to TrkA protein in a DFG-out conformation highlighting key protein-ligand interactions with black dashed lines. B) Co-crystal structure of lead molecule **3** bound to TrkA protein highlighting binding site surface with brown representing hydrophobic regions, green neutral polarity regions, blue polar regions. Some protein residues have been omitted for clarity. PDB code is 6DKW for compound **3**.

**Table 1. Back pocket SAR and associated in vitro data**

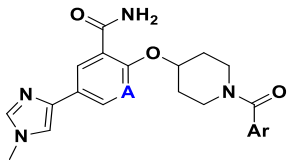


| ID | A | Ar | TrkA cell $IC_{50}$ (μM)[a] | LogD[b] | LipE[c] | HLM[d] | hHep[e] | RRCK $P_{app}$ [f] | P-gp ER | Herg FP $IC_{50}$ (μM)[g] |
|---|---|---|---|---|---|---|---|---|---|---|
| **4** | C | 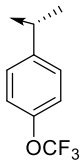 | 0.011 | 3.5 | 4.5 | 31 | ND | 6.2 | 11 | 6.5 |
| **5** | C | 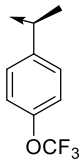 | 0.72 | 3.4 | 2.7 | <8 | ND | 7.7 | 11 | 4.2 |
| **6** | C | 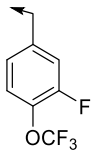 | 0.011 | 3.0 | 5.0 | <8 | 13 | 6.4 | 34 | ND |
| **7** | C | 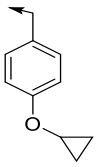 | 0.040 | 2.3 | 5.1 | 23 | ND | 10 | 30 | >40 |
| **8** | N | 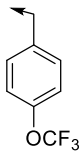 | 0.010 | 2.4 | 5.6 | <8 | 13 | 13 | 10 | 4.5 |

[a]TrkA data were generated in PathHunter cells from DiscoveRx with at least 3 tests on 3 different assay runs.[31] [b]LogD measured at pH 7.4. [c]LipE= -Log(TrkA cell $IC_{50}$) – LogD. [d]Human liver microsome metabolic $CL_{int}$ in mL/min/mg protein.[e]Human hepatocyte $CL_{int}$ in μL/min/million cells.[f]Apparent permeability (x $10^{-6}$ $cms^{-1}$) measured with low efflux MDCKII cell line (RRCK).[35] Data for LogD, HLM, HLMUGT, hHep, RRCK and P-gp were results from at least 2 replicate determinations. [g]hERG FP assay data with at least 2 tests on 2 different assay runs.[32] ND denotes not determined.

Figure 3B shows the binding site surface of ligand **3** when bound to TrkA protein. The binding site surface suggests that the piperidine linker can be further substituted to occupy more of the binding site. Moreover, piperidine substitution may enhance interactions with Phe589 and Phe669 through increased van de Waals interactions and potential CH-π interactions if the piperidine is substituted by an electron withdrawing group. To this end, 3-fluoropiperidine derivatives of the most LipE efficient compound **8** in Table 1, were prepared (Table 2). Both enantiomers of the cis and trans diastereomers were synthesized and gave up to a 3-fold enhancement in TrkA potency and improved LipE by up to 0.4 units when compared with lead molecule **3** (ligand **10b,** LipE 5.7). All compounds were pan-Trk inhibitors with similar potencies at TrkA/B/C (within 3-fold), P-gp and BCRP efflux substrates and exhibited moderate apparent permeability. Ligand **10b** offered the best balance of TrkA potency (TrkA cell $IC_{50}$ 1.9nM, TrkB cell $IC_{50}$ 2.6nM, TrkC cell $IC_{50}$ 1.1nM), LipE, metabolic stability as measured by hHep CLint, and hERG liability as measured by hERG FP (Ligand **10b** hERG FP $IC_{50}$ 14μM). The binding mode of **10b** was established via X-ray crystallography with a 2.68Å co-crystal structure with TrkA protein (Figure 4). Ligand **10b** made similar interactions with TrkA protein to ligand **3** (Figure 3), but had additional van de Waals interactions between F and Phe589. There were also CH-π interactions introduced between the piperidine and Phe589/Phe669. Compound **10b** was screened in 41 biochemical kinase assays (including TrkA) at a concentration of 1μM at Invitrogen for kinase selectivity (see supporting information). Gratifyingly **10b** exhibited superb Trk selectivity with >95% inhibition of TrkA and >40% inhibition of only 1 other kinase VEGFR2, (cell based assay follow-up at Caliper Lifesciences indicated VEGFR2 $IC_{50}$ >5μM). Furthermore, wide ligand profiling of **10b** at a concentration of 10μM in 84 targets to assess off target based liabilities indicated a clean profile

(1 hit with % inhibition >50% at 10μM which gave follow-up alpha1a antagonist $IC_{50}$ 8μM). The exciting in vitro profile of **10b** led to the progression of this compound to in vivo studies.[31]

**Table 2. Piperidine linker SAR and associated in vitro data**

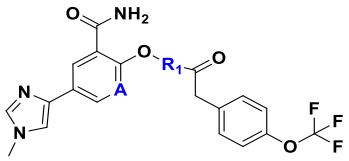


| ID | A | R1 | TrkA cell $IC_{50}$ (nM)[a] | LogD[b] | LipE[c] | HLM[d] | hHep[e] | RRCK $P_{app}$ [f] | P-gp ER | BCRP ER | Herg FP $IC_{50}$ (μM)[g] |
|---|---|---|---|---|---|---|---|---|---|---|---|
| **9a** | N | 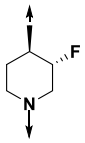 | 74 | 3.0 | 4.1 | <8 | 14 | 11 | 13 | 2.8 | 7.0 |
| **9b** | N | 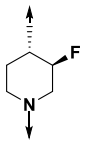 | 5.4 | 3.0 | 5.3 | <8 | 12 | 9 | 14 | 3.3 | 24 |
| **10a** | N | 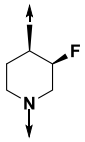 | 3.0 | 3.0 | 5.5 | <8 | 12 | 13 | 10 | 2.5 | 9.0 |
| **10b** | N | 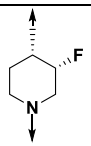 | 1.9 | 3.0 | 5.7 | <8 | 7 | 17 | 10 | 4.6 | 14 |
| **11** | C | 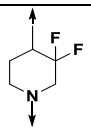 | 2.8 | 3.1 | 5.5 | 24 | 11 | 10 | 13 | ND | ND |

[a]TrkA data were generated in PathHunter cells from DiscoveRx with at least 3 tests on 3 different assay runs.[31] [b]LogD measured at pH 7.4. [c]LipE= -Log(TrkA cell $IC_{50}$) – LogD. [d]Human liver microsome metabolic $CL_{int}$ in mL/min/mg protein.[e]Human hepatocyte $CL_{int}$ in μL/min/million cells.[f]Apparent permeability (x $10^{-6}$ $cms^{-1}$) measured with low efflux MDCKII cell line (RRCK).[35] Data for LogD, HLM, hHep, RRCK, P-gp and BCRP were results from at least 2 replicate determinations. [g]hERG FP assay data with at least 2 tests on 2 different assay runs.[32] ND denotes not determined.

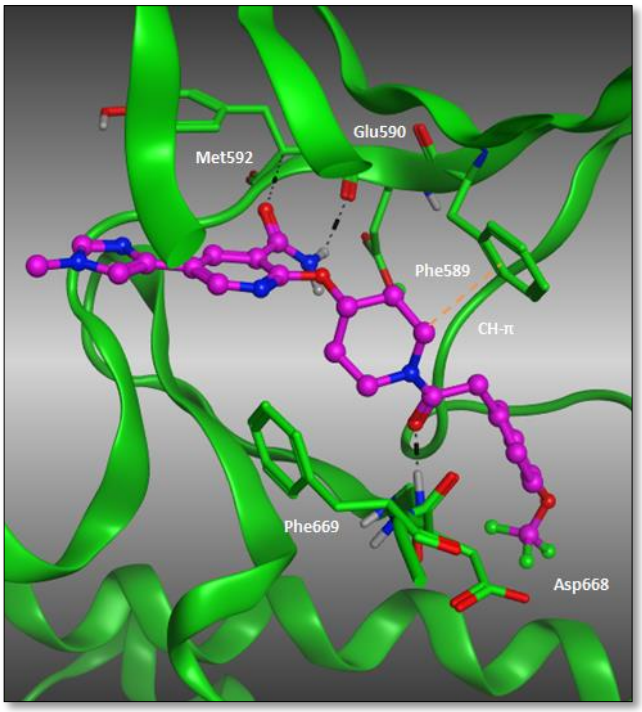


**Figure 4.** Co-crystal structure of ligand **10b** bound to TrkA protein in a DFG-out conformation, highlighting key protein-ligand interactions with black dashed lines. Ligand **10b** shown in magenta and TrkA protein shown in orange. Some protein residues have been omitted for clarity. PDB code is 6DKB for compound **10b**.

**Design of benzamide alcohols as pan-Trk inhibitors**

The co-crystal structure of PF-06273340 with TrkA protein has been published recently by our group.[9, 29] PF-06273340 and **10b** have different hinge binders with the aminopyrimidine of PF-06273340 interacting with the backbone NH and C=O of Met592 whilst the amide in **10b** interacts with the backbone NH of Met592 and backbone C=O of Glu590. Despite this difference an overlay of the ligand bound conformation with TrkA of PF-06273340 and compound **10b** revealed an opportunity to remove the imidazole group in **10b** and append an alcohol moiety heading into the ribose pocket (Figure 5). Keeping both the imidazole and alcohol groups would result in high strain

and high molecular weight. To this end the hybrid ether linked compounds shown in Table 3 were prepared.[36] Gratifyingly, the alcohols **12-14** were active in TrkA cell based assays and also demonstrated a lower hERG liability when compared with the benzamides in Table 2. The cis diastereomers **13a/13b** were 5-50 fold more active than the corresponding trans diastereomers **12a/12b**. The primary alcohol isomer **14** was also active in TrkA cell based assays but showed significantly higher metabolic CL in hHeps possibly due to enhanced metabolism involving the primary alcohol when compared with a tertiary alcohol.[37]

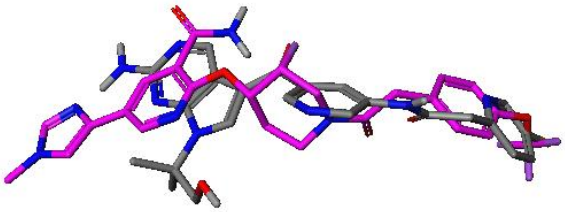

**Figure 5.** Overlay of the bound ligand conformation in TrkA protein of DFG-out binders PF-06273340 (grey) and compound **10b** (magenta).

**Table 3. Benzamide alcohols and associated in vitro data**

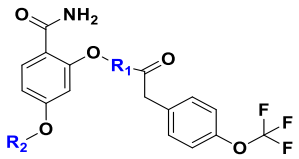


| ID | R1 | R2 | TrkA cell $IC_{50}$ (nM)[a] | LogD[b] | LipE[c] | HLM[d] | hHep[e] | RRCK $P_{app}$ [f] | P-gp ER | BCRP ER | Herg FP $IC_{50}$ (µM)[g] |
|---|---|---|---|---|---|---|---|---|---|---|---|
| **12a** | 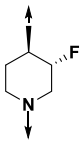 | 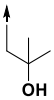 | 410 | 3.1 | 3.3 | <8 | ND | 5.7 | 48 | ND | 29 |
| **12b** | 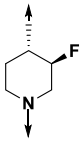 | 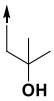 | 61 | 3.0 | 4.2 | <8 | 5.9 | 11 | 22 | ND | 38 |
| **13a** | 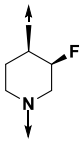 |  | 13 | 3.2 | 4.7 | <8 | 6.1 | 5.4 | 64 | 6.5 | 38 |
| **13b** | 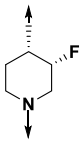 | 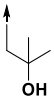 | 7.7 | 3.1 | 5.0 | <8 | 2.0 | 5.2 | 72 | 7.0 | 42 |
| **14** | 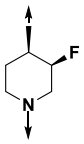 |  | 28 | 3.0 | 4.6 | 11 | 25 | 11 | 22 | ND | 35 |

[a]TrkA data were generated in PathHunter cells from DiscoveRx with at least 3 tests on 3 different assay runs.[36] [b]LogD measured at pH 7.4. [c]LipE= -Log(TrkA cell $IC_{50}$) – LogD. [d]Human liver microsome metabolic $CL_{int}$ in mL/min/mg protein. [e]Human hepatocyte $CL_{int}$ in µL/min/million cells.[f]Apparent permeability (x $10^{-6}$ $cms^{-1}$) measured with low efflux MDCKII cell line (RRCK).[35] Data for LogD, HLM, hHep, RRCK, P-gp and BCRP were results from at least 2 replicate determinations. [g]hERG FP assay data with at least 2 tests on 2 different assay runs.[32] ND denotes not determined.

Benzamide alcohol **13b** offered the best balance of TrkA potency (TrkA cell $IC_{50}$ 7.7nM, TrkB cell $IC_{50}$ 15nM, TrkC cell $IC_{50}$ 3.9nM), LipE, and metabolic stability as determined in hHep ($CL_{int}$ = 2μL/min/$10^6$ cells). The binding mode of **13b** was established via X-ray crystallography with a 2.53Å co-crystal structure with TrkA protein (Figure 6). Ligand **13b** made similar interactions with TrkA to ligand **10b** (Figure 4), however **13b** had additional van de Waals interactions between the gem dimethyl groups and Phe669 and interactions between the alcohol and water molecules towards the kinase exit. Compound **13b** was screened in 42 biochemical kinase assays (including TrkA) at a concentration of 1μM at Invitrogen for kinase selectivity (see supporting information). Gratifyingly **13b** exhibited superb Trk selectivity with >95% inhibition of TrkA with no other kinase being inhibited by >40% at 1μM. Furthermore, wide ligand profiling at a concentration of 10μM at 82 targets to assess off target based liabilities showed a clean profile with no hits having >50% inhibition at 10μM. The exciting in vitro profile of **13b** led to the progression of this compound to in vivo studies.[36]

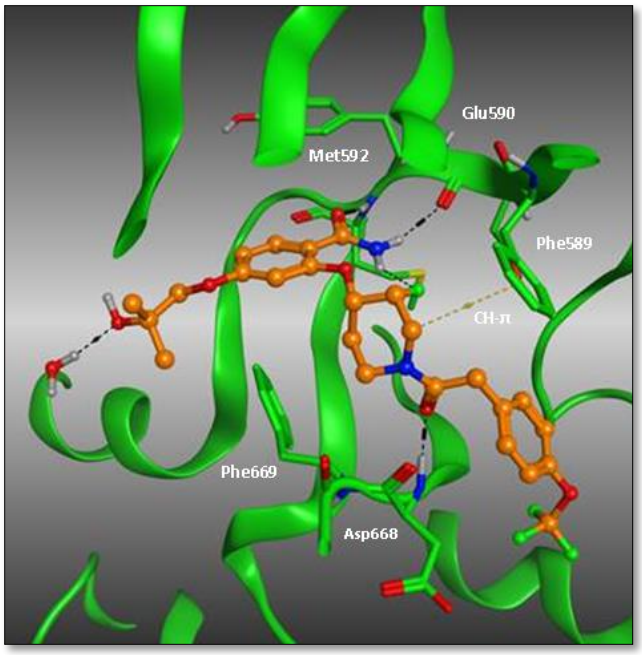


**Figure 6.** Co-crystal structure of ligand **13b** bound to TrkA protein in a DFG-out conformation, highlighting key protein-ligand interactions with black dashed lines. Ligand **13b** shown in orange and TrkA protein shown in green. Some protein residues have been omitted for clarity. PDB code is 6DKG for compound **13b**.

**Design of aminopyridine pan-Trk inhibitors**

Aminopyridines have been described as efficient kinase hinge binding motifs and this concept led to an additional hybrid design wherein the benzamide hinge binder in molecules **2-3** (Figure 2) was changed to an aminopyridine.[38] This hypothesis led to the synthesis of the aminopyridines shown in Figure 7 and Table 4.[39] The aminopyridine in **15** replaces the benzamide hinge binder in ligands **2-3** (Figure 2) and Figure 8 displays an overlay of benzamide **3** when bound to TrkA protein (Figure 3) with aminopyridine **15** docked into TrkA protein. The methyl pyrazole substitution in **15** was thought to be optimal based on the overlay in Figure 8. Aminopyridine **15**

was a potent Trk inhibitor in cell based assays, however replacement of the piperidine ring linker with a pyrrolidine ring during SAR exploration improved TrkA cellular potency by 2-3-fold and LipE by 1 unit in the case of the more active pyrrolidine enantiomer **16b** (Figure 7, TrkA cell $IC_{50}$ 7.7nM, LipE 5.5). Aminopyridines having a pyrrolidine linker were an exciting prospect and further optimisation was conducted on this motif. Based on the learnings with ligand **3** thus far (Figure 2, Table 2) the N-methyl pyrazole unit was replaced by an N-methyl imidazole and fluorinated pyrrolidine derivatives were prepared (Table 4).[39]

**Figure 7.** Generation of aminopyridine pan-Trk inhibitors

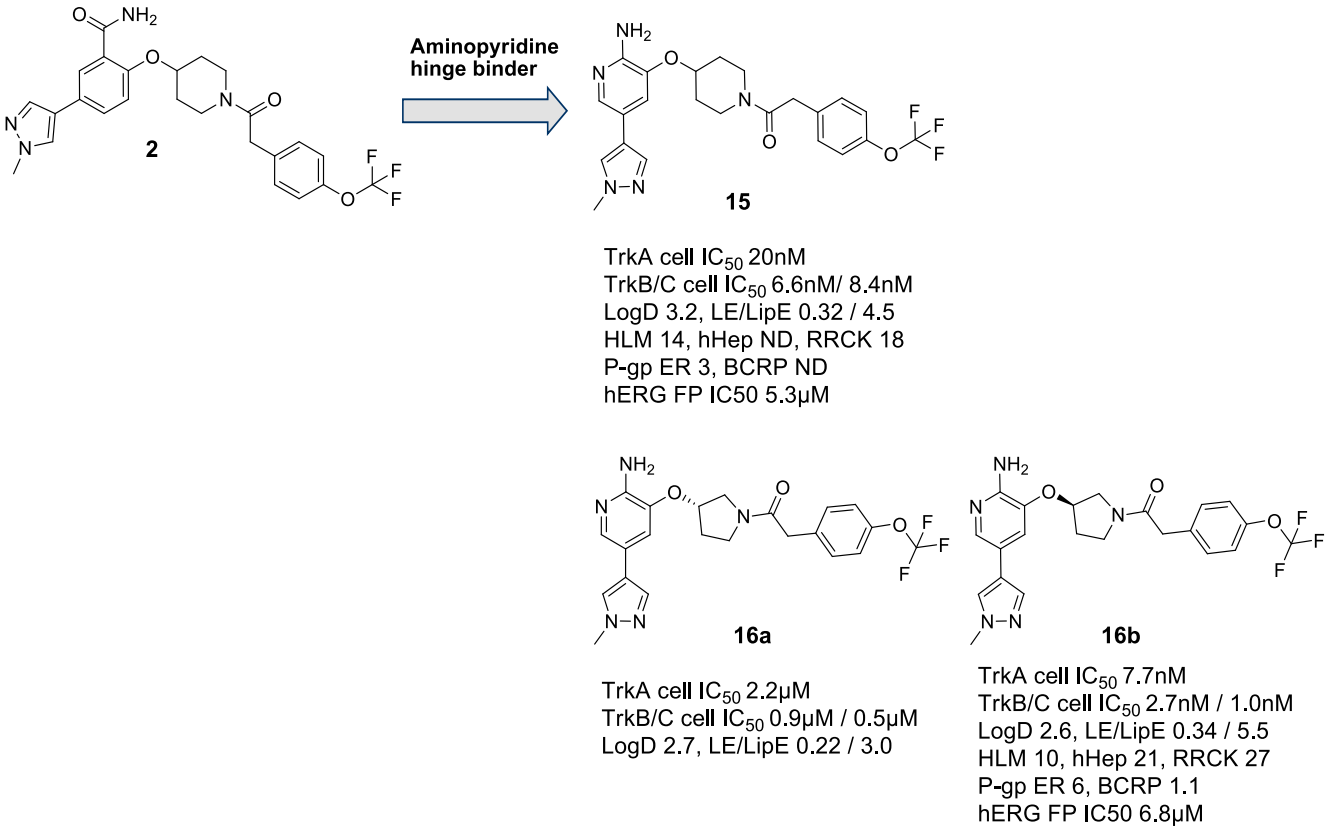

**Table 4. Aminopyridine amides and associated in vitro data**

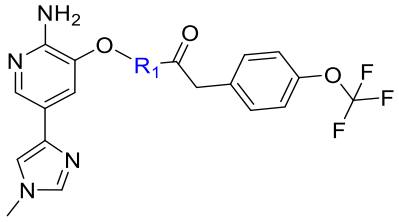

| ID | R1 | TrkA cell $IC_{50}$ (μM)[a] | LogD[b] | LipE[c] | HLM[d] | hHep[e] | RRCK $P_{app}$ [f] | P-gp ER | BCRP ER | Herg FP $IC_{50}$ (μM)[g] |
|---|---|---|---|---|---|---|---|---|---|---|
| **17a** | 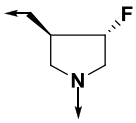 | 1.1 | 2.6 | 3.4 | 15 | ND | 17 | 10 | ND | 16 |
| **17b** | 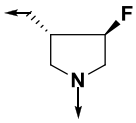 | 0.008 | 2.6 | 5.5 | <8 | 17 | 22 | 12 | ND | 15 |
| **18a** | 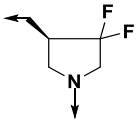 | 1.8 | 2.8 | 2.9 | 9.1 | ND | 22 | 12 | ND | 21 |
| **18b** | 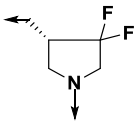 | 0.001 | 2.8 | 6.2 | 9.7 | 9.1 | 22 | 13 | 5.0 | 11 |

[a]TrkA data were generated in PathHunter cells from DiscoveRx with at least 3 tests on 3 different assay runs.[39] [b]LogD measured at pH 7.4. [c]LipE= -Log(TrkA cell $IC_{50}$) – LogD. [d]Human liver microsome metabolic $CL_{int}$ in mL/min/mg protein. [e]Human hepatocyte $CL_{int}$ in μL/min/million cells.[f]Apparent permeability (x $10^{-6}$ $cms^{-1}$) measured with low efflux MDCKII cell line (RRCK).[35] Data for LogD, HLM, hHep, RRCK, P-gp and BCRP were results from at least 2 replicate determinations. [g]hERG FP assay data with at least 2 tests on 2 different assay runs.[32] ND denotes not determined.

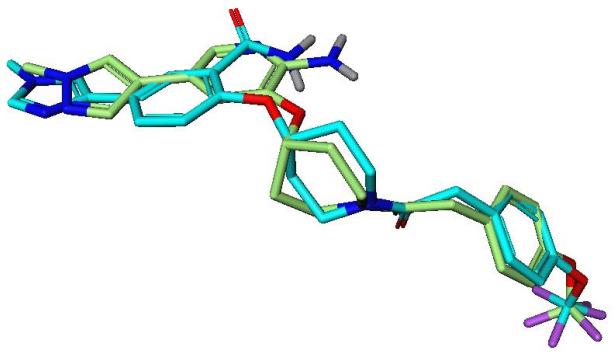

**Figure 8.** Overlay of the bound ligand conformation in TrkA protein of lead molecule **3** (blue, Figure 3) and aminopyridine **15** docked into TrkA protein.

Mono and difluorinated pyrrolidines (Table 4) were potent TrkA inhibitors with 100-1000-fold preference of TrkA for the more potent enantiomers (**17b, 18b**) over the weaker enantiomers (**17a, 18a**). Cis monofluorinated derivatives proved more challenging to synthesize than the corresponding trans monofluorinated isomers. Difluorinated pyrrolidine **18b** was 8-fold more active when compared with the monofluorinated derivative **17b** possibly due to enhanced van der Waals interactions. Moreover **18b** exhibited greater metabolic stability than **17b** as measured by hHep $Cl_{int}$ (**17b** and **18b** hHep $CL_{int}$ = 17 and 9.1μL/min/$10^6$ cells respectively) conceivably due to blocking of oxidative metabolism by the additional F in **18b**. Metabolite identification studies in hHeps with **16b** (Figure 7, data not shown) indicated the major metabolism pathways involved N-demethylation, pyrrolidine unit oxidation and glucuronidation on the amino moiety. Ligand **18b** was active in the hERG FP and PX assay (hERG FP $IC_{50}$ 14μM, hERG PX $IC_{50}$ 7.7μM) although **18b** had a good therapeutic index (TI) for TrkA over hERG due to its nanomolar potency at TrkA. Based on the SAR developed to date the imidazole substituent in **18b** could be replaced as demonstrated by the benzamide alcohols in Table 3. Moreover, amides are well established

bioisosteres for heterocycles and hence an amide substituent was introduced in place of the imidazole moiety in **18b** to give amides **19** and **20** (Figure 9). Methyl amide **19** was a potent and LipE efficient TrkA inhibitor (TrkA cell $IC_{50}$ 8.4nM, LipE 5.6) with low metabolic turnover in human in vitro assays (HLM <8μL/min/mg protein, hHep 1.4μL/min/million cells). Moreover **19** demonstrated excellent selectivity over hERG in the hERG FP assay ($IC_{50}$ 79μM) and hERG PX assay ($IC_{50}$ 88μM). Ethyl amide **20** was also a potent TrkA inhibitor (TrkA cell $IC_{50}$ 10nM, LipE 5.2) although it offered no advantage over **19** and had a LipE that was ~0.4 units lower than **19**. This relatively flat SAR was consistent with the terminal amide occupying a region of TrkA that exits the kinase towards solvent, much like the imidazole group in Figure 3. Ligand **19** seemed to offer the best balance of TrkA potency, LipE, metabolic stability and hERG liability when compared with **18b** (Table 4) and was chosen for further progression. The binding mode of **19** was determined via X-ray crystallography with a 2.11Å co-crystal structure with TrkA protein (Figure 10). The aminopyridine group did indeed act as a hinge binder with the amino unit NH interacting with the main chain C=O of Glu590 and the pyridyl N interacting with the main chain Met592 NH. The terminal amide had a vector towards the solvent exposed kinase exit and appeared to interact with water. The pyrrolidine linker exhibited van der Waals interactions with the surrounding residues such as Phe669, Phe589, Val524 along with potential CH-π interactions with Phe589 and Phe669. Consistent with the previous TrkA co-crystal structures discussed (Figures 3-4, and 6) the central amide carbonyl of **19** formed a hydrogen bond with the main chain NH of Asp668 and the p-$OCF_3$ phenyl group occupied the back pocket.

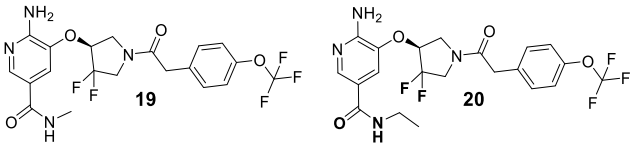


| 19 | 20 |
|---|---|
| TrkA cell $IC_{50}$ 8.4nM | TrkA cell $IC_{50}$ 10nM |
| TrkB/C cell $IC_{50}$ 6.2nM / 2.2nM | TrkB/C cell $IC_{50}$ ND |
| LogD 2.5, LE/LipE 0.34 / 5.6 | LogD 2.8, LE/LipE 0.33 / 5.2 |
| HLM <8, hHep 1.4, RRCK 11 | HLM <8, hHep 3.4, RRCK14 |
| P-gp ER 22, BCRP ER 4 | P-gp ER 22, BCRP ND |
| hERG FP / PX $IC_{50}$ 79μM / 88μM | hERG FP / PX $IC_{50}$ 43μM / ND |

**Figure 9.** Discovery of aminopyridine amide **19**

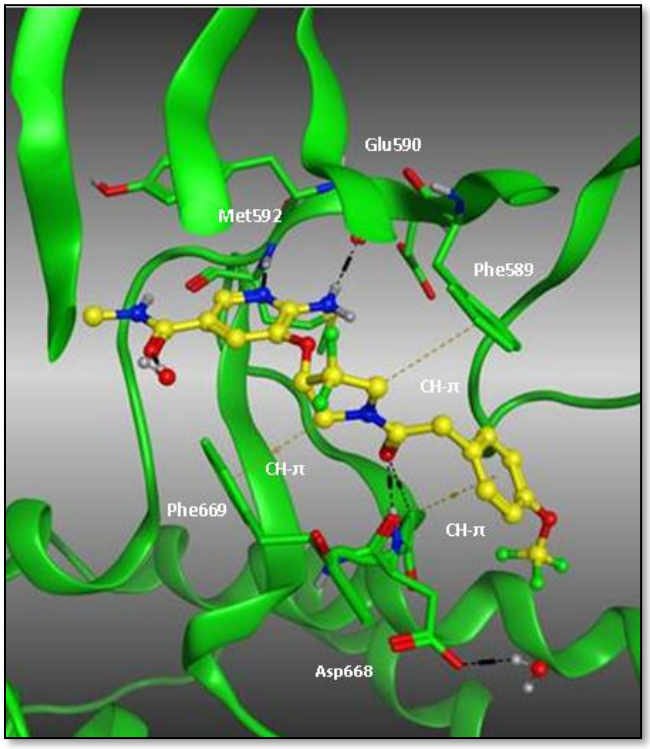


**Figure 10.** Co-crystal structure of aminopyridine **19** bound to TrkA protein in a DFG-out conformation, highlighting key protein-ligand interactions with black dashed lines. Ligand **19** shown in yellow and TrkA protein shown in green. Some protein residues have been omitted for clarity. PDB code is 6DKI for compound **19**.

Compound **19** was screened at 44 biochemical kinase assays (including TrkA) at a concentration of 1μM at Invitrogen for kinase selectivity (see supporting information). Ligand **19** exhibited outstanding Trk selectivity with >95% inhibition of TrkA with no other kinase being inhibited by >40% at 1μM. Furthermore, wide ligand profiling to assess off target based liabilities at a concentration of 10μM in 82 targets indicated a clean profile with no hits having >50% inhibition at 10μM. The exciting in vitro profile of **19** led to the progression of this compound to in vivo studies.[39]

**Surface plasmon resonance data for pan-Trk ligands 10b, 13b and 19**

Ligands **10b, 13b** and **19** were evaluated using surface plasmon resonance with immobilised TrkA protein (residues 441-796). With non-activated unphosphorylated TrkA protein, ligands **10b, 13b** and **19** demonstrated relatively slow association and dissociation kinetics,[40] with measured $K_D$ values consistent with TrkA cellular potencies **10b**: $K_a$ 6.9x10$^5$ M$^{-1}$s$^{-1}$ , $K_d$ 4.7 x10$^{-4}$ s$^{-1}$, $K_D$ 0.7 nM; **13b**: $K_a$ 4.4 x10$^4$ M$^{-1}$s$^{-1}$, $K_d$ 1.1 x10$^{-4}$ s$^{-1}$, $K_D$ 2.6 nM; **19**: $K_a$ 5.7 x10$^4$ M$^{-1}$s$^{-1}$, $K_d$ 1.3 x10$^{-4}$ s$^{-1}$, $K_D$ 2.3 nM.

**In vivo rat PK data for pan-Trk ligands 10b, 13b and 19**

The optimized pan-Trk ligands **10b, 13b** and **19** were examined in oral and i.v. PK studies in rats where they demonstrated low systemic CL and moderate oral bioavailability that was consistent with good absorption (Table 5). These compounds were also found to be peripherally restricted with $C_{b,u}/C_{p,u}$ of <0.05 in all cases in CNS penetration studies in rat. These in vivo data confirm that in these optimized pan-Trk ligands, acceptable oral absorption and restriction from the CNS can be combined. These properties that are demonstrated in rats are desirable in pan-Trk inhibitors

intended for use as oral medicines for chronic pain, and can be reasonably expected to translate to human.

**Table 5. Compounds 10b, 13b and 19: pharmacokinetic properties in rat**

| | i.v. administration | | | | | p.o. administration | | |
|---|---|---|---|---|---|---|---|---|
| **ID** | **dose (mg/Kg)** | **T½ (hr)** | **plasma CL (mL/min/Kg)** | **Vss (L/Kg)** | **$C_{b,u}/C_{p,u}$** | **dose (mg/Kg)** | **Tmax (hr)** | **Oral F (%)** |
| **10b** | 1 | 2.6 | 13.4 | 0.65 | 0.043 | 3 | 0.5 | 52 |
| **13b** | 1 | 1.9 | 8.9 | 0.6 | 0.026 | 3 | 0.5 | 35 |
| **19** | 1 | 3.9 | 18.5 | 1.4 | 0.018 | 3 | 0.6 | 56 |

Compounds were administered via intravenous (i.v.) and oral (p.o.) routes to separate groups of two male rats. $C_{b,u}/C_{p,u}$ was determined separately following i.v. infusion in 4 male rats. Further details of PK and CNS penetration experiments are given in the supporting information.

**Predicted human clearance of pan-Trk ligands 10b, 13b and 19**

Metabolic pathways of **10b**, **13b** and **19** were examined in HLM and in hHep in vitro (see supporting information). In HLM, metabolism of all three analogues was identified as occurring through pathways consistent with CYP-mediated oxidation. In separate incubations of compounds in human liver cytosol fraction, disappearance of compounds over time was undetectable. Thus, the pattern of metabolite formation and absence of detectable turnover in human liver cytosol suggested that AO was not involved in metabolism of these compounds. In hHep, the benzamides **10b** and **13b** were found to form some of the oxidized metabolites detected in HLM, without evidence of phase 2 conjugation pathways. The aminopyridine **19** also formed oxidized

metabolites in hHep but also formed small amounts of glucuronidated products, consistent with conjugation at the aminopyridine moiety. In the absence of metabolism by AO, prediction of systemic CL in human by scaling in vitro metabolic turnover data can be performed with higher confidence than previously possible for the development candidate pan-Trk inhibitor PF-06273340. Turnover of analogues **10b**, **13b** and **19** in HLM was too low to be quantified (<8μL/min/mg), whereas in hHep, $CL_{int}$ was measurable using the 'relay' assay technique designed for compounds exhibiting high metabolic stability.[41] $CL_{int}$ values were 7.8, 2.0 and 1.4 μL/min/$10^6$ cells, for **10b**, **13b** and **19**, respectively, which scaled to systemic plasma CL values in human of 1.5, 0.3 and 0.6 mL/min/Kg, respectively, consistent with minimal hepatic extraction.

**Solubility of pan-Trk ligands 10b, 13b and 19**

Solubility is a drug property that plays a key role in the development potential and PK profile of clinical candidates.[34, 42] The solubility of our previous development candidate PF-06273340 was low for the crystalline form at approximately 2μg/mL in a pH 6.5 aqueous phosphate buffer. In comparison the solubility of **10b**, **13b** and **19** was significantly higher 15, 76, and 55μg/mL respectively. This improvement in solubility can be attributed to, in part, the higher fraction of sp3 hybridised carbons of **10b**, **13b** and **19** when compared with PF-06273340, and fewer HBDs in **10b**, **13b** and **19** when compared with PF-06273340 that can result in high lattice energies (PF-06273340.[43-44] Ligands **10b** and **19** gave highest measured pKa values (between 4.2-4.7). The improved solubility of **10b**, **13b** and **19** gave further confidence in the clinical development potential of these analogues.

**In vivo efficacy in UV burn hyperalgesia models**

Compounds **10b**, **13b** and **19** were assessed in the UV irradiation-induced thermal hyperalgesia (UVIH) model of inflammatory pain in rats whereby their effects on thermal hyperalgesia resulting from UV irradiation were determined by measuring paw withdrawal latency (PWL) (Figure 11). Single oral doses of **10b** (0.03, 0.32 and 3 mg/Kg), **13b** (0.15, 1.5 and 15mg/Kg) and **19** (0.03, 0.32 and 3 mg/Kg) were administered 48 hours after UV treatment and PWL measured at 1, 3 and 6 hours post dose. The doses of compounds were chosen in order to achieve multiples of TrkA cell $IC_{50}$ of 0.1x, 1.0x and 10x at some time between 1 and 6 hours. The effect on hyperalgesia of all three compounds at the highest dose studied is shown in Figure 11 and their effects at all doses administered are summarized in Table 6. All three compounds significantly reversed hyperalgesia at the highest two doses employed at each of the time-points studied ($p<0.05$, 2-way ANOVA vs. vehicle). The positive control ibuprofen (100mg/Kg, p.o.) also reversed thermal hyperalgesia at the 1 and 3 hour time-points (individual compound dose response data compared with vehicle and positive control ibuprofen for **10b**, **13b** and **19** is provided in the supporting information). Whilst no effect on PWL was observed at any dose of **10b** or **19** for the contralateral hindpaw, the highest dose of **13b** displayed a significant effect on contralateral PWL ($P<0.05$, data not shown). Unbound plasma concentrations of compounds were determined in animals at 6 hours post dose. This demonstrated that statistically significant efficacy was observed at unbound plasma concentrations equivalent to the following multiples of TrkA cell $IC_{50}$: **10b**: 0.5x (0.03mg/Kg), 4x (3mg/Kg); **13b**: 0.8x (0.15mg/Kg), 13x (15mg/Kg); **19**: 0.15x (0.3mg/Kg), 2x (3mg/Kg). Overall, it is possible to say that in these experiments, efficacy was achieved at doses of compounds that corresponded with unbound exposure at multiples of TrkA cell $IC_{50}$ of 2x – 13x.

**Table 6. Effects of 10b, 13b and 19 on UV irradiation-induced hyperalgesia in rats**

| ID | dose (mg/Kg) | significance of difference from vehicle | | |
|---|---|---|---|---|
| | | 1h | 3h | 6h |
| **10b** | 0.03 | N.S. | p<0.05 | N.S. |
| | 0.3 | p<0.001 | p<0.001 | p<0.001 |
| | 3 | p<0.001 | p<0.001 | p<0.001 |
| **13b** | 0.15 | N.S. | p<0.05 | N.S. |
| | 1.5 | p<0.001 | p<0.001 | p<0.001 |
| | 15 | p<0.001 | p<0.001 | p<0.001 |
| **19** | 0.03 | N.S. | N.S. | N.S. |
| | 0.3 | p<0.05 | p<0.001 | p<0.05 |
| | 3 | p<0.001 | p<0.001 | p<0.001 |

The statistical significance of effects on PWL (ipsilateral paw, n = 8) were determined according to 2-way ANOVA vs. vehicle data (N.S = not significant (p>0.05)). Dose response data compared with vehicle and positive control ibuprofen for **10b**, **13b** and **19** are provided in the supporting information.

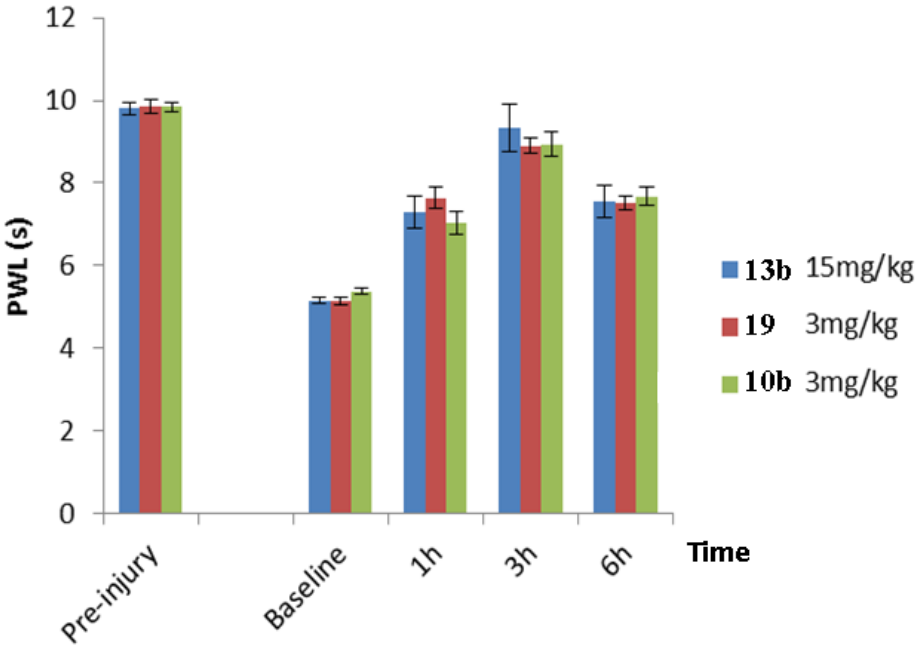


**Figure 11.** Effects of compounds **10b**, **13b** and **19** in the UVIH model in rats at the highest dose studied. Ipsilateral paw data are shown, n=8 rats per dose group. Statistical significance according to 2-way ANOVA vs. vehicle data is given in Table 6. Dose response data compared with vehicle and positive control ibuprofen for **10b**, **13b** and **19** is provided in the supporting information.

Ligands **10b**, **13b** and **19** were progressed to either 2 week (ligands **10b** and **19**) or 4 week (**13b**) exploratory toxicity studies in rat. No adverse effects (including behavioral) were observed at free average concentrations ($C_{avg}$) of 725x, 882x and 133x TrkA cell $IC_{50}$ for **10b**, **19** and **13b** respectively. Moreover **10b**, **19** and **13b** exhibited a favorable genetoxicity profile suitable for advancement.

**Free energy based computational methods**

The availability of computational methods that can reliably, rapidly, and accurately predict the binding affinities of ligands to a target protein of interest would greatly facilitate SBDD. To this end we have recently described a collaborative study that compares TrkA binding affinity predictions using two free energy based methods: Enhanced Sampling of Molecular dynamics with Approximation of Continuum Solvent (ESMACS) and Thermodynamic Integration with Enhanced Sampling (TIES), to experimentally derived TrkA binding affinities for a set of Pfizer pan-Trk compounds.[45] Individual binding affinities were calculated in a few hours, exhibiting good correlations with the experimental data of 0.79 and 0.88 from the ESMACS and TIES approaches, respectively. We are now in the process of expanding the pan-Trk dataset used to include the compounds in this manuscript and further explore these methods. Moreover, recent developments in conformational sampling of a binding site such as REST (Replica Exchange with Solute Tempering) and/or REST2 will be combined with ESMACS and TIES to provide further enhancement in potency prediction accuracy.[46-47] The results of these ongoing studies will be reported in due course.

**Chemistry**

A typical synthetic route towards the pyrazole compounds **1** and **2** is described in Scheme 1. Phenol **21** was alkylated by displacement of mesylate **22** with cesium carbonate in DMF to afford **23**. A Suzuki reaction with N-methyl pyrazole boronate ester **24**, followed by hydrolysis of the nitrile with potassium hydroxide produced benzamide **26**. The Boc group was deprotected with HCl leading to piperidine **27**. Urea compound **1** was then formed by reacting **27** with isocyanate

**28** using pyridine as the base. Amide **2** was formed via reaction of **27** with phenyl acetic acid **29** using HATU and DIPEA.

**Scheme 1.** Synthesis of hit molecule **2** and lead molecule **3** via mesylate displacement and Suzuki coupling methodology[a]

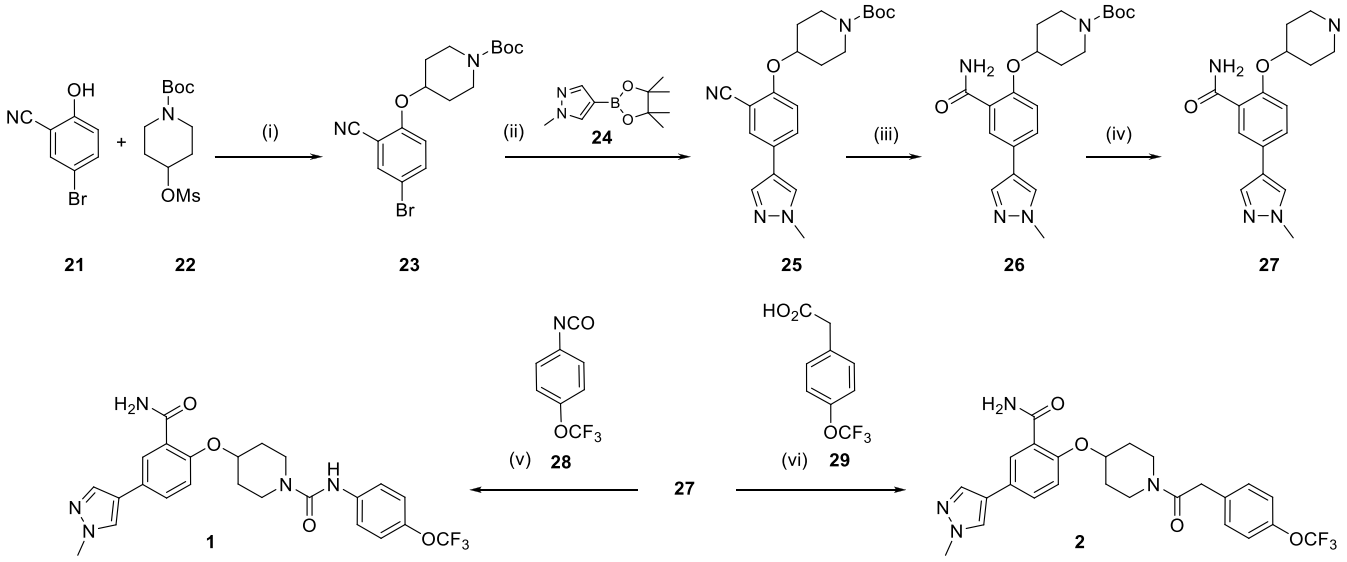


[a]Reagents and conditions: (i) $Cs_2CO_3$, DMF, 65%; (ii) **24**, $Pd(PPh_3)_2Cl_2$, $Cs_2CO_3$, >99%; (iii) KOH, tBuOH, 96%; (iv) HCl, >99%; (v) **28**, pyridine, 73%; (vi) **29**, HATU, DIPEA, DMF, 40%.

The synthesis of phenyl acetic acid derivatives from Table 1 are described in Scheme 2. Aryl bromide **30** was converted to the boronate ester **31** through palladium mediated coupling with $B_2Pin_2$. Subsequent Suzuki-Miyaura coupling was performed with the bromoimidazole **32** to give **33**. Piperidine **35** was synthesized via mesylate displacement and deprotection and then coupled with a range of substituted phenyl acetic acids under HATU or EDC conditions to give the desired compounds **3**, **4**, **5**, **6**, and **7**.

**Scheme 2.** Synthesis of phenyl acetic acid derivatives via Suzuki coupling, mesylate displacement and amide coupling methodology[a]

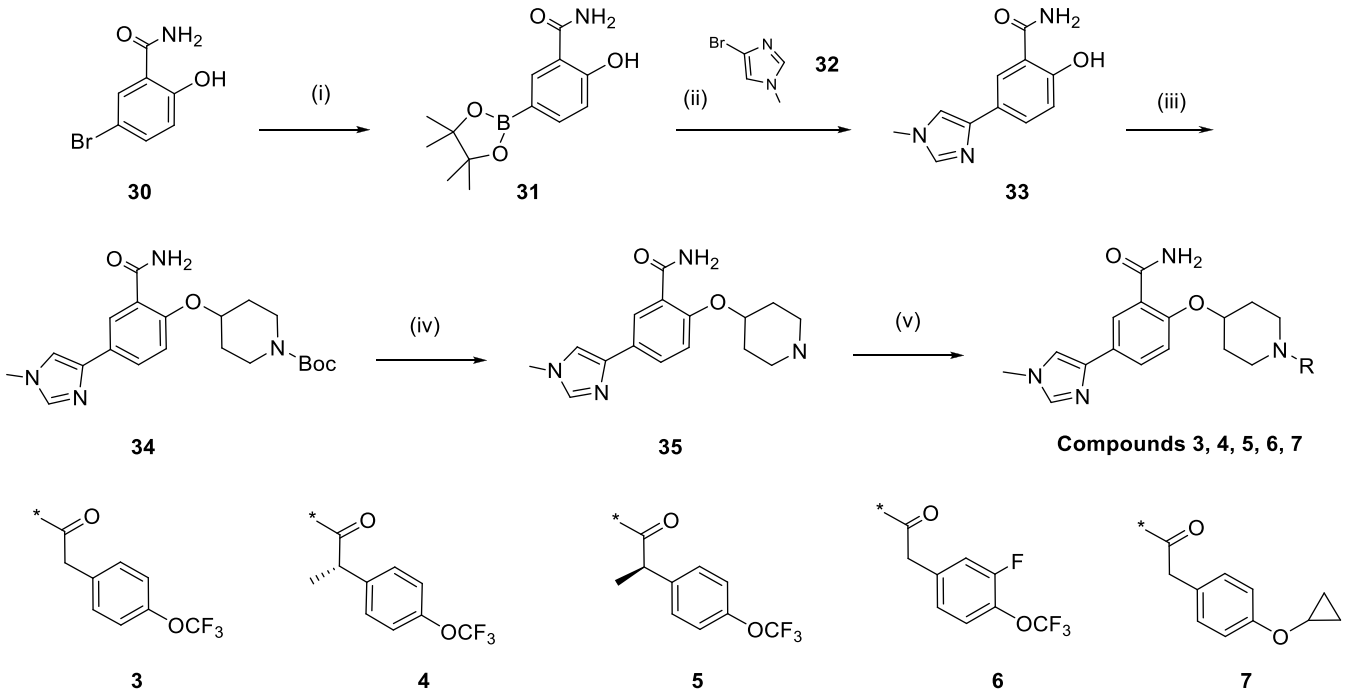


[a]Reagents and conditions: (i) $B_2Pin_2$, $PdCl_2$(dppf)-DCM, KOAc, dioxane 100°C, 16h, 44%; (ii) **32**, $Pd_2(dba)_3$, $(t\text{-}Bu)_3PHBF_4$, $Na_2CO_3$, dioxane-$H_2O$, 100°C, 16h, 68%; (iii) **22**, $Cs_2CO_3$, DMF, (49%); (iv) HCl/dioxane, >99%; (v) HATU or EDC coupling.

Scheme 3 illustrates the preparation of a range of piperidines to give compounds **8, 9a, 9b, 10a,** and **10b.** In this sequence, the substituted piperidines (shown in Table 2) were installed early in the synthesis followed by subsequent Suzuki-Miyaura reaction using iodoimidazole **42**. $S_NAr$ reaction of commercial Boc protected fluoropiperidinol **36**,[48] with 2-chloropyridine **37** occurred in high yield using potassium t-butoxide as base in DMSO at room temperature to give **38**. Removal of the Boc group was followed by HATU coupling with phenyl acetic acid to give bromopyridine **40**. **40** was converted to the boronate ester and Suzuki coupled with **42** give the desired compounds in Table 2.

**Scheme 3.** Synthesis of fluoropiperidine derivatives in **Table 2**[a]

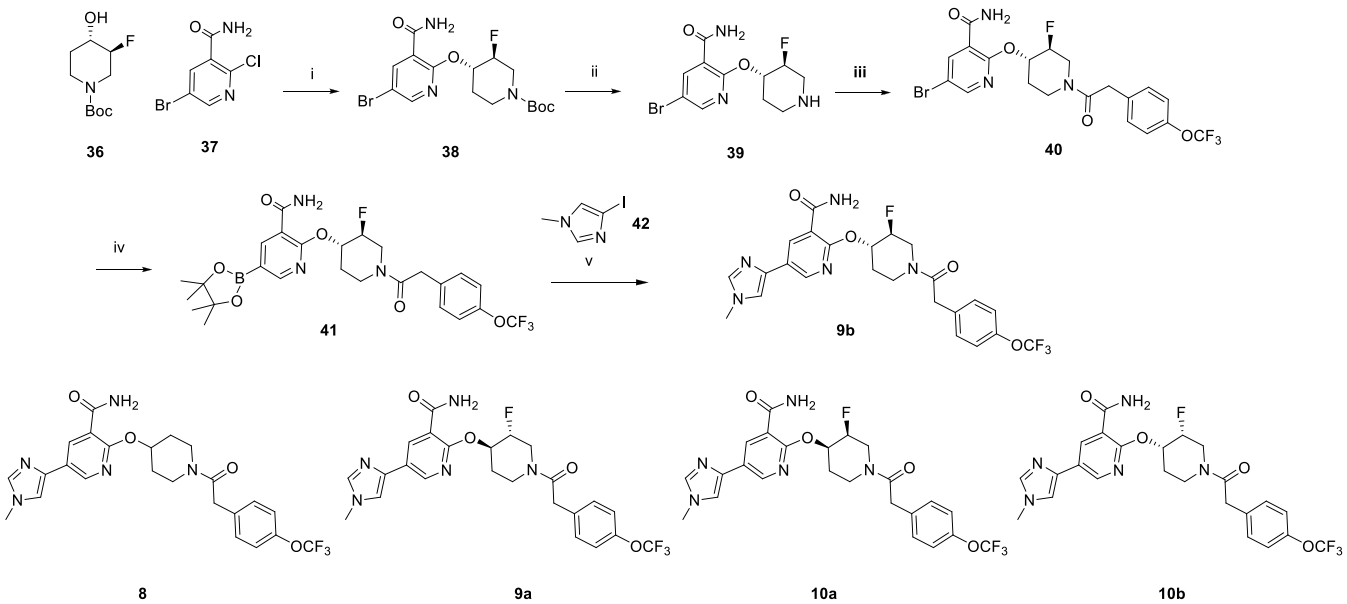


[a]Reagents and conditions: (i) **37**, KOtBu, DMSO, room temperature, 16h, 72%; (ii) HCl/dioxane, >99%; (iii) **29**, HATU, TEA, DMF, 93%; (iv) $B_2Pin_2$, $PdCl_2$(dppf).DCM, KOAc, dioxane, 100ºC, 16h, 61%; (v) **42**, $PdCl_2$(dppf), $K_2CO_3$, DMF-water, 100ºC, 16h, 24%.

Compound **45** was prepared using SnAr conditions at an elevated temperature of 100 ºC with gem-difluoro piperidinol **43** and fluoro aryl **44** (Scheme 4). Conversion to the boronate ester **46** and Suzuki-Miyaura coupling with bromoimidazole **32** led to product **47**. Boc-deprotection and coupling with acid **29** using COMU gave 81% yield of compound **11**.

**Scheme 4.** Synthesis of difluoropiperidine derivative **11**[a]

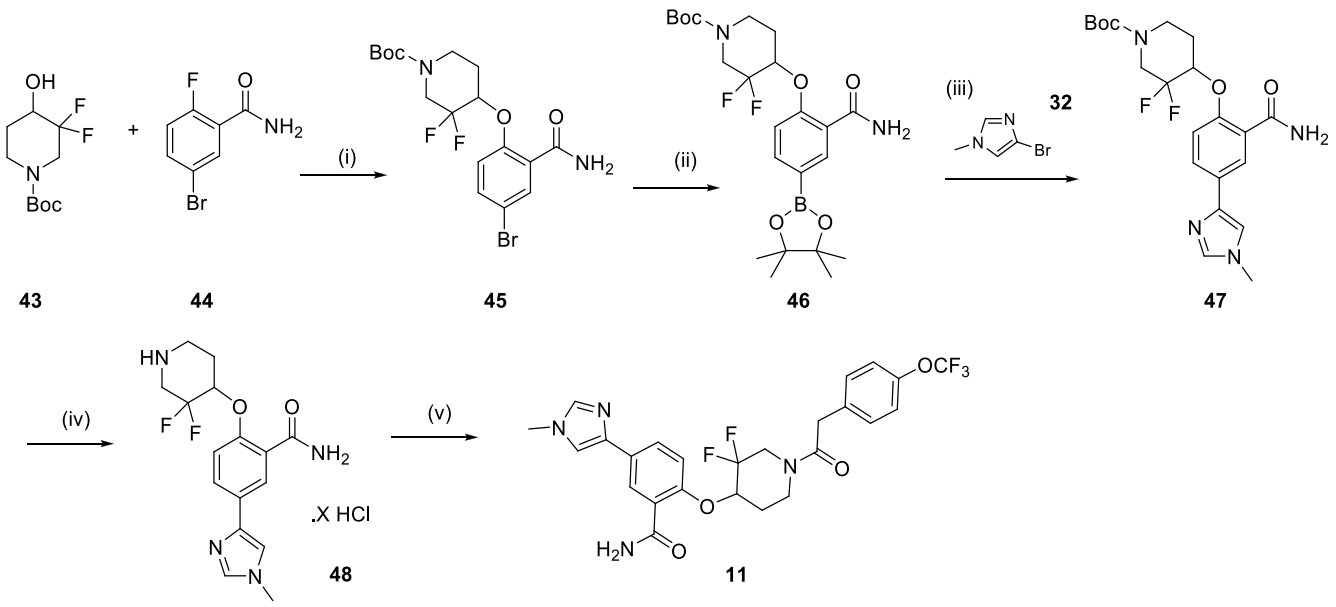


[a]Reagents and conditions: (i) $Cs_2CO_3$, DMF, 100ºC, 24h, 90%; (ii) $B_2pin_2$, KOAc, $PdCl_2$(dppf), dioxane, 100ºC 16h, >99%; (iii) **32**, $Pd_2dba_3$, $tBu_3PH.BF_4$ $Na_2CO_3$ (aq) dioxane, 100ºC 18h, 25%; (iv) HCl/dioxane, >99%; (v) **29**, COMU, DIEA, DMF, room temperature, 14h, 81%.

The standard preparation towards tertiary alcohols, shown in Table 3, is described in Scheme 5 producing the four compounds **12a**, **12b**, **13a**, and **13b**. A variety of fluoro substituted piperidines were used in the $S_NAr$ reaction with aryl fluoride **49** using cesium carbonate as base and DMF as solvent at 100 ºC to give ether **51** (as an example towards **13b**). Hydrolysis of the nitrile using basic conditions afforded benzamide **52**, which was then deprotected to give piperidine **53**. Phenyl acetic acid **29** was coupled using EDC conditions to give amide **54**. Hydrogenation of the benzyl ether revealed phenol **55** which was treated with isobutylene oxide under thermal conditions to give the desired tertiary alcohols shown in Scheme 5.

**Scheme 5.** Synthesis of tertiary alcohol derivatives in **Table 3**[a]

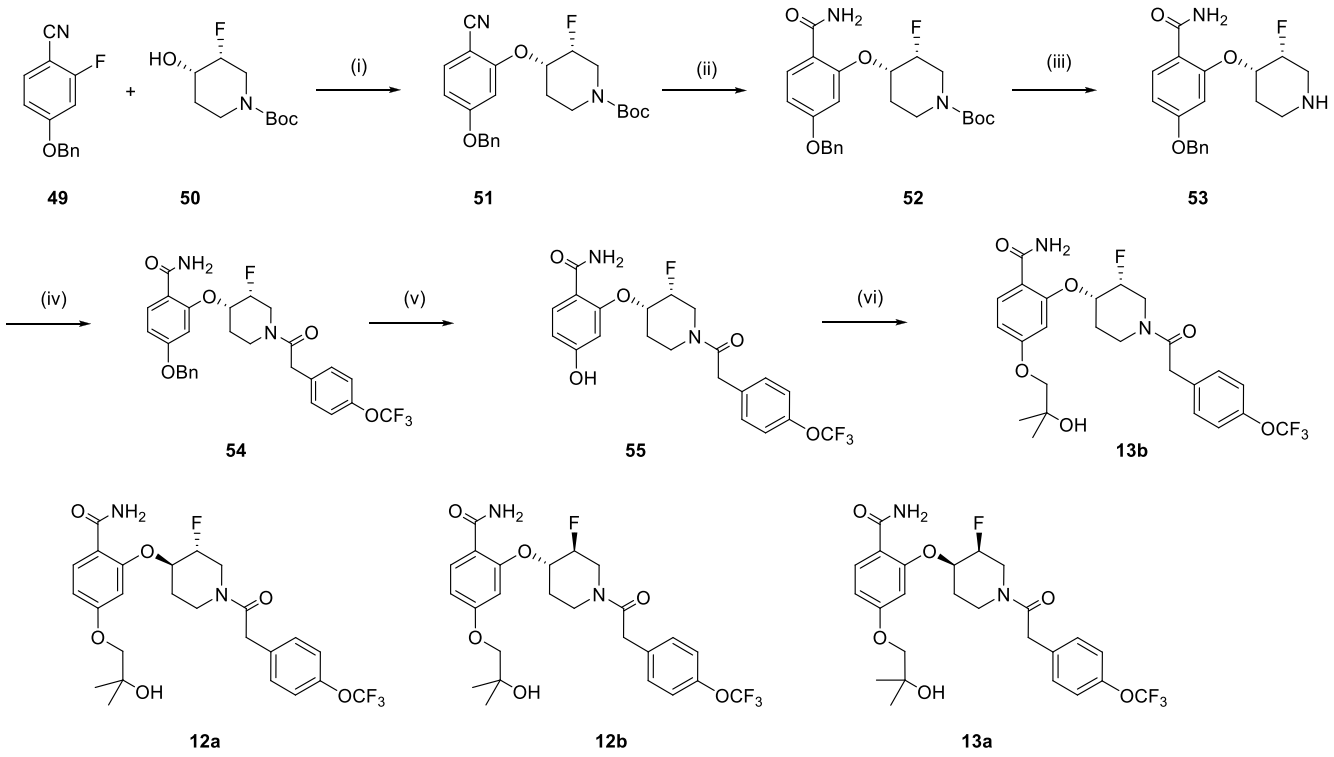


[a]Reagents and conditions: (i) $Cs_2CO_3$, DMF, 100ºC, 16h, 90%; (ii) KOH, tBuOH, 80ºC, 16h, 51%; (iii) HCl/dioxane, >99%; (iv) **29**, EDC, HOBt, DIPEA, 16h, 82%; (v) $H_2$ (balloon), Pd/C, EtOH, 2h, room temperature, 93%; (vi) isobutylene oxide, $K_2CO_3$, DMF, 100ºC, 16h, 26%.

To prepare primary alcohol **14** (Scheme 6), phenol **56** was treated with 2-bromo-2-methyl propionic acid to give gem-dimethyl ether **57**. Saponification to the acid **58**, followed by *in situ* generation of a mixed anhydride and reduction with $NaBH_4$ afforded the corresponding alcohol **14**.

**Scheme 6.** Synthesis of primary alcohol **14**[a]

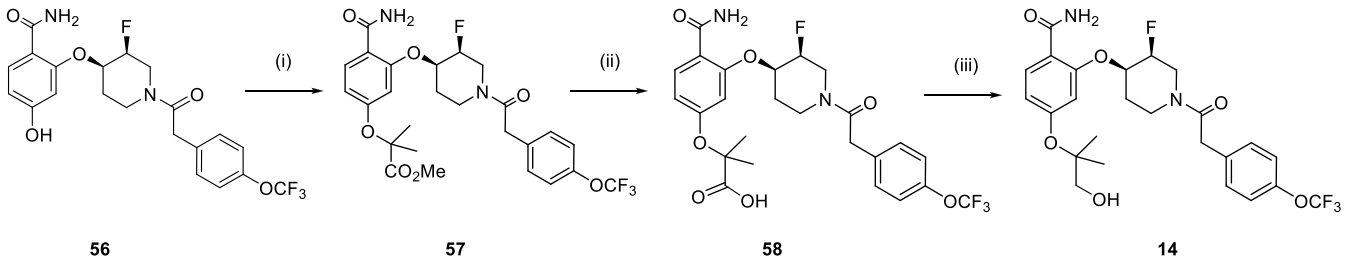


[a]Reagents and conditions: (i) 2-bromo-2-methyl proprionic acid, $Cs_2CO_3$, DMF, 100°C, 16h, 98%; (ii) LiOH, THF-water, room temperature, 4h, 82%; (iii) isobutyl chloroformate, then $NaBH_4$, 51%;

A typical synthetic route to compounds **15, 16a**, and **16b** (Figure 7, Table 4) is described in Scheme 7. Heteroaryl bromide **59** was subjected to Suzuki-Miyaura coupling conditions with the N-methyl-pyrazole boronate ester to give excellent yields of the pyrazole product **60**.[49-50] Deprotection with sodium hydroxide and methanol revealed the 2-amino-3-hydroxy pyridine **61**, which was then treated with (S)-pyrrolidine mesylate to give ether **63**. Similar Boc deprotection and coupling conditions allowed the generation of compounds **15**, **16a**, and **16b**.

**Scheme 7.** Synthetic route towards compounds **15, 16a**, and **16b**[a]

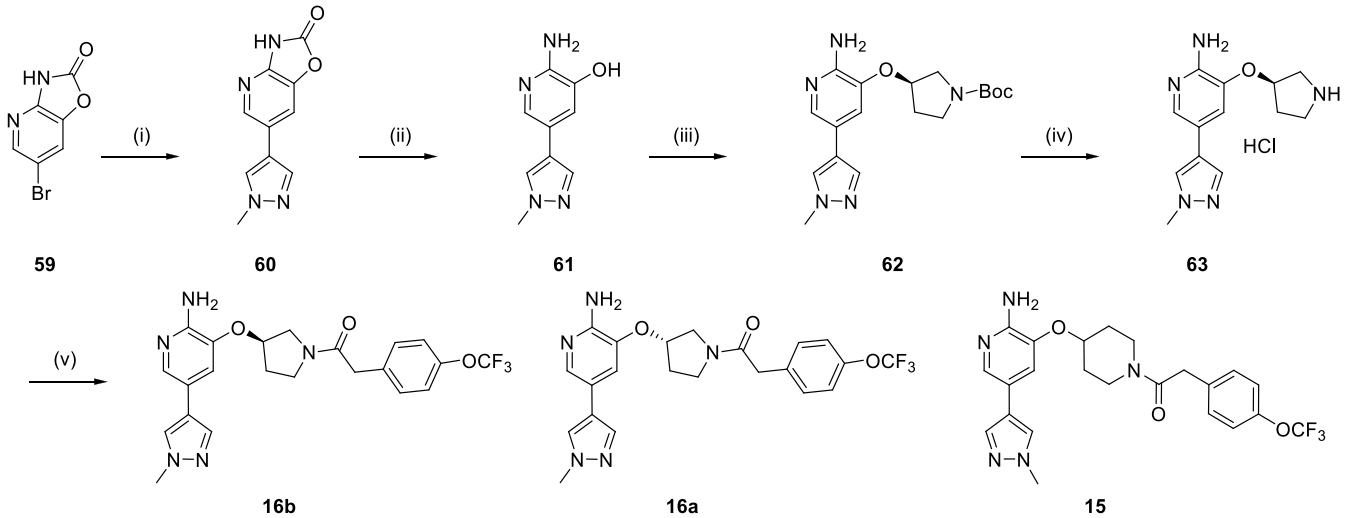


[a]Reagents and conditions: (i) **24**, $PdCl_2$(dppf), $Na_2CO_3$, dioxane-$H_2O$, 90°C, 90%; (ii) NaOH, MeOH-$H_2O$, reflux, 72%; (iii) (S)-tert-butyl 3-((methylsulfonyl)oxy)pyrrolidine-1-carboxylate, $Cs_2CO_3$, DMF, 85°C, 52%; (iv) HCl/dioxane, >99%; (v) **29**, coupling with HATU or T3P, 21-73%.

Scheme 8 details the synthesis of compounds **17a** and **17b** (Table 4), which were prepared as a racemic mixture, then separated by chiral chromatography. Epoxide opening of **64** with HF at 115°C gave the racemic trans alcohol **(±)65**. Mitsunobu reaction with nitrobenzoic acid gave ester **(±)66** which was hydrolysed to afford cis alcohol **(±)67**. This was converted to triflate **(±)68** which was used for an ether formation with 2-amino-3-hydoxy **71** (prepared in two steps using a Suzuki reaction coupling first with iodoimidazole **42** followed by hydrogenolysis of the benzyl group).[49] After deprotection of **(±)72** and coupling with phenyl acetic acid, the racemic material was purified by chiral chromatography to give the two enantiomers **17a** and **17b**.

**Scheme 8.** Synthetic route towards compounds **17a** and **17b**[a]

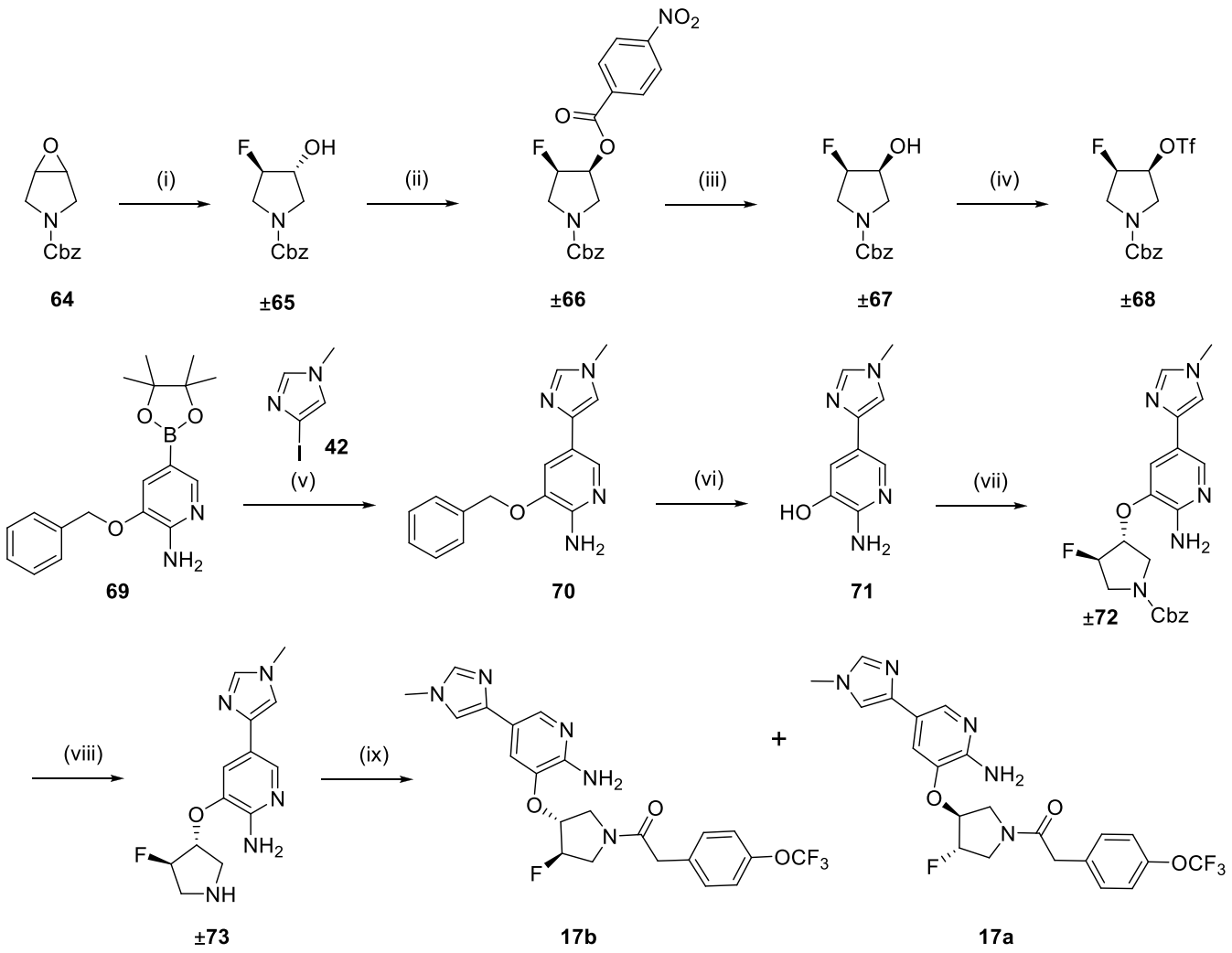


[a]Reagents and conditions: (i) HF.TEA, 115ºC, 81%; (ii) p-nitrobenzoic acid, DIAD, $PPh_3$, THF; (iii) 1N NaOH, THF, 57% (over 2 steps); (iv) $Tf_2O$, pyridine, DCM, 91%; (v) **42**, Pd(dppf)$Cl_2$.DCM, $K_2CO_3$, DMF, 69%,; (vi) $H_2$, Pd$(OH)_2$/C, EtOH, 88%; (vii) **±68**, $Cs_2$CO3, DMF room temperature, 63%; (viii) 33% HBr/AcOH, DCM, >99%; (ix) **29**, HATU, DIEA, then chiral SFC separation, 44%.

Compounds **18a** and **18b** were also prepared in a racemic synthesis (Table 4, Scheme 9). 3-Fluoro pyridine **75** underwent $S_NAr$ reaction with racemic gem-difluoro pyrrolidine **74** using cesium carbonate in THF to afford excellent yields of ether **76**. Reduction of the nitropyridine via hydrogenation over palladium on carbon gave amine **77**. Subsequent bromination with NBS gave bromopyridine **78** and the imidazole was installed via a Stille reaction with imidazole stannane **79**. Following deprotection, coupling, and separation of enantiomers, the single enantiomers **18a** and **18b** were generated.

**Scheme 9.** Synthetic route towards compounds **18a** and **18b**[a]

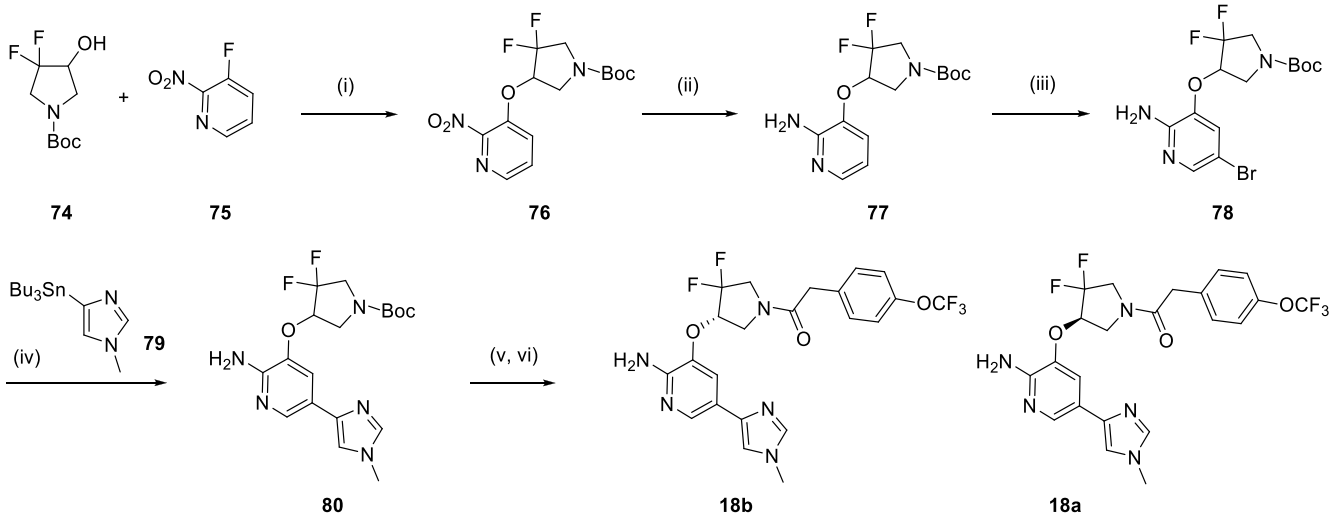


[a]Reagents and conditions: (i) $Cs_2CO_3$, THF, 91%; (ii) $H_2$, Pd/C, MeOH, >99%; (iii) NBS, DMF, 82%; (iv) **79**, $PdCl_2(PPh_3)_2$, DMF, 120°C, 90%; (v) TFA; (vi) **29**, HATU, TEA, DMF, then chiral SFC separation (35% each enantiomer over 2 steps).

Using intermediate **78** from Scheme 9, a palladium-catalyzed carbonylation under pressure in the presence of methanol afforded ester **81** (Figure 9, Scheme 10). Amide **82** was prepared using standard deprotection and coupling conditions. Methyl and ethyl amides **19** and **20** were then

synthesized by saponification of the alkyl ester to acid **83** followed by coupling of the primary methyl and ethyl amines. Chiral separation gave the separate enantiomers.

**Scheme 10.** Synthetic route towards compounds **19** and **20**[a]

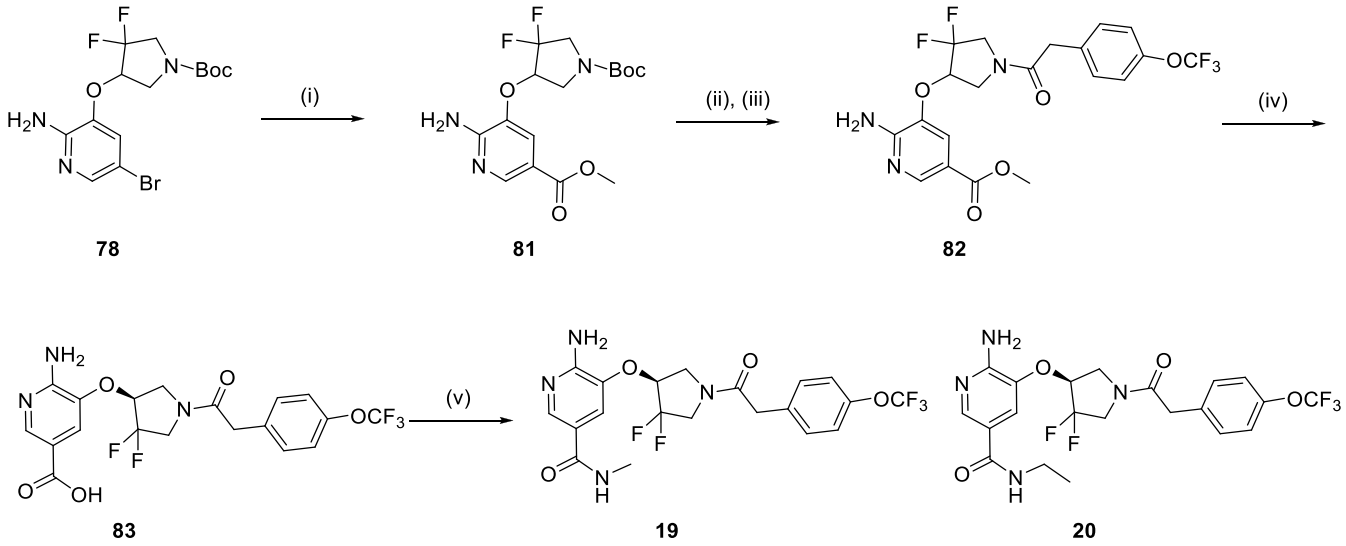


[a]Reagents and conditions: (i) CO (5.2 bar), $Pd(OAc)_2$, DPPF, $Et_3N$, MeOH, DMF, 80°C, 65%; (ii) TFA (iii) **29**, HATU, TEA, DMF, 95% (over 2 steps), (iv) NaOH, MeOH, >99%; (v) $MeNH_2$-HCl or $EtNH_2$-HCl, HATU, TEA, then chiral SFC separation.

## CONCLUSION

Based on the clinical efficacy of NGF neutralizing antibodies in inflammatory pain there is substantial interest in the advancement of small molecule inhibitors of TrkA for the treatment of pain. Our current pan-Trk (TrkA, TrkB, TrkC) inhibitor development candidate PF-06273340 was found to be metabolized via AO-catalyzed reactions leading to a potential clearance prediction liability and contingency pan-Trk candidates were sought, whereby AO-mediated metabolism was avoided in order to mitigate human pharmacokinetic risk. Thus, three candidate quality pan-Trk

compounds that have high confidence in human PK prediction were designed **10b, 13b** and **19**. Ligand **10b** was delivered by optimizing hit molecule **1** which was discovered by analysis of the in-house kinase selectivity dataset. Candidate molecule **13b** was designed as a hybrid between development candidate PF-06273340 and **10b**, wherein the solvent exposed groups were interchanged. Hinge binder and linker modification then led to candidate molecule **19**. All three compounds were predicted to possess low metabolic clearance in human that does not proceed via AO-catalyzed reactions, thus addressing the potential clearance prediction liability associated with PF-06273340. Moreover, the high potency, off target selectivity, in vivo toxicity profile along with absorption, peripheral restriction, and human CL predictions made all three pan-Trk inhibitors exciting and promising structurally differentiated assets suitable for advancement into a variety of clinical pain studies.

## EXPERIMENTAL SECTION

**General.** $^{1}$H Nuclear magnetic resonance (NMR) spectra were in all cases consistent with the proposed structures. Characteristic chemical shifts (δ) are given in parts-per-million (ppm) (δ relative to residual solvent peak) using conventional abbreviations for designation of major peaks: *e.g.* s, singlet; d, doublet; t, triplet; m, multiplet; br, broad. The mass spectra (*m/z*) were recorded electrospray ionization. The following abbreviations have been used for common solvents: $CDCl_3$, deuterochloroform; DMSO-$d_6$, deuterodimethylsulfoxide; $CD_3OD$, deuteromethanol. All solvents were reagent grade and, when necessary, were purified and dried by standard methods. Concentration of solutions after reactions and extractions involved the use of a rotary evaporator operating at a reduced pressure of ca. 20 Torr. Anhydrous solvents were obtained from commercial sources and used as is. The chemical yields reported below are unoptimized. Purity criteria: Final compounds isolated as singletons >95% based on LCMS and/or HPLC. The experimental

procedures for all of the steps in the synthesis of all target compounds can be found in Pfizer patent applications WO2015092610, WO2016009296 and WO2016020784.

**4-(2-carbamoyl-4-(1-methyl-1H-pyrazol-4-yl)phenoxy)-N-(4-(trifluoromethoxy)phenyl)piperidine-1-carboxamide (1).** 5-bromo-2-hydroxybenzonitrile **21** (20 g, 101.10 mmol) and tert-butyl 4-((methylsulfonyl)oxy)piperidine-1-carboxylate **22** (33.8 g, 121.21 mmol) were combined in dry DME (400 mL, 0.25 M). $Cs_2CO_3$ (40g, 121.21 mmol) was added and the reaction was heated to 100 $^oC$ for 24 hours. The reaction was cooled to room temperature and water was added and the reaction extracted with EtOAc. The organics were washed with water, dried over $Na_2SO_4$, filtered and concentrated. The crude material was purified by $SiO_2$ column chromatography to afford **23** (25 g, 65%). LCMS [M+1-tBu] 325.0; $^1$HNMR (400 MHz, d-DMSO) δ ppm 8.00 (s, 1H), 7.82 (m, 1H), 7.33 (d, J = 9.12 Hz, 1H), 4.82 (m, 1H), 3.55 (m, 2H), 3.29 (m, 2H), 1.90 (m, 2H), 1.63 (m, 2H), 1.45 (s, 9H). Compound **23** (24 g, 62.9 mmol) and 1-methyl-4-(4,4,5,5-tetramethyl-1,3,2-dioxaborolan-2-yl)-1H-pyrazole **24** (15.72 g, 75.7 mmol) was added to DMF (314 mL, 0.2M). $Cs_2CO_3$ (61.5 g, 188.9 mmol) in water (88.4 mL) was added to the reaction mixture and the mixture purged with $N_2$ for 1 hour. $Pd(PPh_3)_2Cl_2$ (2.5g 3.14 mmol) was then added and the reaction heated to 80 $^oC$ for 16 hours. The reaction mixture was concentrated to remove most of the solvent, then water and DCM were added. The reaction was extracted with DCM and the organic layer washed with water, brine, and dried over $Na_2SO_4$. The organic layer was filtered, concentrated, and purified by $SiO_2$ column chromatography with EtOAc/Hexanes to obtain **25** (24 g, >99%). LCMS [M+1] 383.2; $^1$HNMR (400 MHz, d-DMSO) δ ppm 8.15 (s, 1H), 7.94 (d, J = 1.72 Hz, 1H), 7.89 (s, 1H), 7.81 (m, 1H), 7.33 (d, J = 8.88, 1H), 4.79 (m, 1H), 3.85 (s, 3H), 3.57 (m, 2H), 3.30 (m, 2H), 1.90 (m, 2H), 1.62 (m, 2H), 1.41, (s, 9H).

*General hydrolysis procedures A*. To compound **25** (2.5 g, 6.54 mmol) in tBuOH (25 mL, 0.26M) was added KOH (732 mg, 13.08 mmol). The reaction mixture was heated to 80 ºC for 16 hours. The reaction was cooled to room temperature and EtOAc and water were added. The organic layer was washed with brine, dried over $Na_2SO_4$, filtered and concentrated to give **26** (2.5 g, 96%) and used directly in the next step. LCMS [M+1] 401.2; $^1$HNMR (400 MHz, d-DMSO) δ ppm 8.10 (s, 1H), 7.87 (d, J = 1.8 Hz, 1H), 7.79 (s, 1H), 7.61 (m, 1H), 7.54 (bs, 2H), 7.19 (d, J = 8.64 Hz, 1H), 3.84 (s, 3H), 3.62 (m, 2H), 3.23 (m, 2H), 1.90 (m, 2H), 1.63 (m, 2H), 1.41 (s, 9H). *General HCl deprotection procedures B*. To compound **26** (2.5 g, 6.25 mmol) in dioxane (10 mL, 0.63M) was added 4M HCl/dioxane (25 mL). The reaction was stirred for 2 hours at room temperature, then concentrated *in vacuo*. Ether was added and stirred for 10 min. The solid was filtered and washed with ether to give **27** (HCl salt, 2.3g, >99%). LCMS [M+1] 301.4; $^1$HNMR (400 MHz, d-DMSO) δ ppm 9.07 (bs, 1H), 8.89 (bs, 1H), 8.11 (s, 1H), 7.81 (s, 1H), 7.77 (d, J = 2.36 Hz, 1H), 7.59 (m, 3H), 7.18 (d, J = 8.76 Hz, 1H), 4. 78 (m, 1H), 3.85 (s, 3H), 3.20 (m, 2H), 3.08 (m, 2H), 2.11 (m, 2H), 1.93 (m, 2H). A mixture of **27** (80 mg, 0.20 mmol) and 1-isocyanato-4-(trifluoromethoxy)benzene **28** (62.2 mg, 0.306 mmol) in 2 mL of pyridine was stirred at room temperature for 4 hours. To the reaction was added an additional 1.5 eq of 1-isocyanato-4-(trifluoromethoxy)benzene **28** (62.2 mg, 0.306 mmol), and the mixture stirred at room temperature overnight. The reaction was evaporated with toluene and the residue was purified by ISCO (40 g, MeOH/DCM = 0 to 10 %) to give **1** (75 mg, 73%) as a white solid. LCMS ES+ AP+ 504 [M+H], ES- AP+ 502 [M-H]; $^1$H NMR (400 MHz, d-DMSO) δ ppm 8.75 (s, 1H), 8.10 (s, 1H), 7.89 (d, J=2.3 Hz, 1H), 7.80 (s, 1H), 7.61 (dd, J=2.5, 8.6 Hz, 1H), 7.59 - 7.53 (m, 4H), 7.23 (d, J=8.8 Hz, 3H), 4.82 - 4.74 (m, 1H), 3.85 (s, 3H), 3.82 - 3.72 (m, 2H), 3.40 - 3.32 (m, 2H), 2.05 - 1.93 (m,

2H), 1.80 - 1.64 (m, 2H); HRMS for $C_{24}H_{25}F_3N_5O_4$ MS m/z $[M+H]^+$ Calcd: 504.1853, Found 504.1853.

**5-(1-methyl-1H-pyrazol-4-yl)-2-((1-(2-(4-(trifluoromethoxy)phenyl)acetyl)piperidin-4-yl)oxy)benzamide (2).** See procedures for compound **1** steps 1-4, then the following HATU coupling procedures. *General HATU coupling procedures C*. DIPEA (0.793 mL, 4.45 mmol) was added to compound **27** (300 mg, 0.891 mmol) in DMF (5 mL, 0.18M) and stirred for 10 minutes. To this reaction mixture was added 2-(4-(trifluoromethoxy)phenyl)acetic acid **29** (196 mg, 0.89 mmol) and HATU (508 mg, 1.33 mmol) and the mixture stirred at room temperature for 16 hours. The reaction was diluted with water and extracted with EtOAc. The organic layer was washed with water, brine, dried over $Na_2SO_4$, filtered and concentrated. The crude material was purified by $SiO_2$ column chromatography to afford **2** (180 mg, 40%). LCMS [M+1] 503.2; $^1$H NMR (400 MHz, d-DMSO) δ ppm 8.10 (s, 1H), 7.86 (d, J = 2.32, 1H), 7.79 (s, 1H), 7.60 (dd, J = 8.52, 2.34 Hz, 1H), 7.54 (m, 2H), 7.35 (d, J = 8.68 Hz, 2H), 7.30 (d, 8.24 Hz, 2H), 7.20 (d, J = 8.72 Hz, 1H), 4.77 (m, 1H), 3.85 (s, 3H), 3.79 (s, 2H), 3.75 (m, 2H), 3.43 (m, 2H), 1.90 (m, 2H), 1.63 (m, 2H); HRMS for $C_{25}H_{25}F_3N_4O_4$ MS m/z [M] Calcd: 502.1828, Found 502.1832.

**5-(1-methyl-1H-imidazol-4-yl)-2-((1-(2-(4-(trifluoromethoxy)phenyl)acetyl)piperidin-4-yl)oxy)benzamide (3).** *General $B_2Pin_2$ procedures D*. A solution of 5-bromo-2-hydroxybenzamide **30** (25 g, 115.72 mmol), $B_2Pin_2$ (44g, 173.58 mmol) and freshly dried KOAc (34g, 347.17 mmol) in dioxane (500 mL) was degassed with argon for about 20 min. $Pd(dppf)Cl_2$-DCM (2.83g, 3.47mmol) was added and the resulting reaction mixture was heated at 100°C for 16 hours. The reaction mixture was cooled to room temperature and filtered through celite and washed with EtOAc (1 L). Organics were neutralized with 2N HCl and washed with water (200 mL) and brine (200 mL), dried over $Na_2SO_4$, and concentrated under reduced pressure. The crude

compound was purified by triturating with ether, hexane and n-heptane to afford **31** as light brown solid (12 g, 40%). LCMS [M+1] 264.2; $^1$H NMR (400 MHz, d-DMSO) δ ppm 13.45 (s, 1H), 8.55 (bs, 1H), 8.17 (s, 1H), 7.69 (bs, 1H), 7.67 (d, J = 8.24 Hz, 1H), 6.87 (d, J = 8.24 Hz, 1H), 1.29 (s, 12H). *General Suzuki procedures E*. A stirred solution of **31** (12.0 g, 45.63 mmol), **32** (7.35 g, 45.63 mmol) and $Na_2CO_3$ (12.1 g, 114.07 mmol) in dioxane-$H_2O$ (4:1, 200 mL) was degassed with argon for about 20 min. $Pd_2(dba)_3$ (2.09 g, 2.28 mmol) and $tBu_3PHBF_4$ (265 mg, 0.913 mmol) was added and the resulting reaction mixture was heated at 100 °C for 16 hours. The reaction mixture was cooled to room temperature, and concentrated under reduced pressure. The concentrated residue was acidified to pH 5-6 by 6N HCl and filtered through celite and washed with 5% MeOH-DCM (1 L), then with 10% MeOH-DCM + 2% $NH_4OH$ (1 L) and the filtrate was concentrated to afford **33** as a brown solid (6.6 g, 67%). LCMS [M+1] 218.4; $^1$H NMR (400 MHz, d-DMSO) δ ppm 12.89 (s, 1H), 8.46 (bs, 1H), 8.19 (d, J = 1.8 Hz, 1H), 7.87 (bs, 1H), 7.77 (dd, J = 8.56, 1.74 Hz, 1H), 7.63 (s, 1H), 7.44 (s, 1H), 6.86 (d, J = 8.48, 1H), 3.68 (s, 3H). To a solution of **33** (120 mg, 0.55 mmol) and **22** (185 mg, 0.66 mmol) in DMF (3 mL, 0.18M) was added $Cs_2CO_3$ (216 mg, 0.66 mmol) and the mixture stirred at 90 $^o$C for 4 hours. The reaction mixture was cooled to room temperature and diluted with water. The mixture was extracted with EtOAc and the combined organics were washed with water (4 x 50 mL), brine, dried over $Na_2SO_4$, filtered and concentrated. The crude material was purified by $SiO_2$ column chromatography (3-4% MeOH/DCM) to afford **34** as a solid (110 mg, 50%). LCMS [M+1] 401.2; $^1$H NMR (400 MHz, d-DMSO) δ ppm 8.11 (d, J = 2.28 Hz, 1H), 7.77 (dd, J = 8.52, 2.28 Hz, 1H), 7.60 (s, 1H), 7.54 (s, 1H), 7.51 (m, 2H), 7.18 (d, J = 8.72 Hz, 1H), 4.70 (m, 1H), 3.67 (s, 3H), 3.62 (m, 2H), 3.22 (m, 2H), 1.99 (m, 2H), 1.64 (m, 2H), 1.41 (s, 9H). Compound **35** was prepared using general HCl deprotection procedures **B** with **34** (100 mg, 0.25 mmol) to afford an off white solid of **35** (HCl salt, 90 mg, >99%). LCMS

[M+1] 301.2; $^1$H NMR (400 MHz, d-DMSO) δ ppm 9.15 (s, 1H), 9.07 (bs, 1H), 8.83 (bs, 1H), 8.16 (s, 1H), 8.06 (d, J = 2.04 Hz, 1H), 7.90 (dd, J = 8.64, 1.92 Hz, 1H), 7.70 (bs, 1H), 7.61 (bs, 1H), 7.38 (d, J = 8.8 Hz, 1H), 4.88 (m, 1H), 3.88 (s, 3H), 3.22 (m, 2H), 3.11 (m, 2H), 2.14 (m, 2H), 1.95 (m, 2H). *General EDC coupling procedures F.* TEA (11.29 mL, 80.43 mmol) was added to a suspension of **35** (6 g, 16.09 mmol) in DCM (140 mL) and stirred for 10 mins. To this EDCI (4.63 g, 24.13 mmol), HOBT (3.26 g, 24.13 mmol) and **29** (3.54 g, 16.09 mmol) were added and the resulting mixture was stirred for 16 hours at room temperature. The reaction mixture was diluted with water and extracted with DCM. The combined organic layers were washed with $NaHCO_3$ (sat aq), water and brine. The organics were then dried over $Na_2SO_4$ and concentrated to afford crude material that was purified by column chromatography (100-200 $SiO_2$, 3-4% MeOH/DCM) to afford solid compound **3** as an off white solid (4.5 g, 56%). LCMS [M+1] 503.2; $^1$H NMR (400 MHz, d-DMSO) δ ppm 8.10 (d, J=2.4 Hz, 1H), 7.77 (dd, J=2.4, 8.8 Hz, 1H), 7.60 (s, 1H), 7.54 (s, 1H), 7.52 (br. s., 2H), 7.36 (d, J=8.8 Hz, 2H), 7.30 (d, J=8.3 Hz, 2H), 7.19 (d, J=8.8 Hz, 1H), 4.83 - 4.71 (m, 1H), 3.86 - 3.81 (m, J=5.9 Hz, 1H), 3.79 (s, 2H), 3.77 - 3.71 (m, 1H), 3.67 (s, 3H), 3.49 - 3.37 (m, 1H), 3.37 - 3.34 (m, 1H), 1.98 - 1.85 (m, 2H), 1.74 - 1.55 (m, 2H); HRMS for $C_{25}H_{26}F_3N_4O_4$ MS m/z $[M+H]^+$ Calcd 503.1901, found 503.1908.

**(S)-5-(1-methyl-1H-imidazol-4-yl)-2-((1-(2-(4-(trifluoromethoxy)phenyl)propanoyl)piperidin-4-yl)oxy)benzamide (4).** See procedures for compound **3**, then using general EDC coupling procedures **F** and appropriate carboxylic acid, then chiral separation of enantiomers: LCMS [M+1] 517.6; $^1$H NMR (400 MHz, d-DMSO) δ ppm 8.07 (dd, J=2.2, 11.0 Hz, 1H), 7.74 (d, J=8.3 Hz, 1H), 7.59 (s, 1H), 7.53 (s, 2H), 7.46 - 7.36 (m, 3H), 7.34 - 7.30 (m, 2H), 7.14 (d, J=8.8 Hz, 1H), 4.68 (br. s., 1H), 4.31 - 4.18 (m, 1H), 3.94 - 3.67 (m, 2H), 3.66 (s, 3H), 3.47 - 3.35 (m, 1H), 3.29 - 3.18 (m, 1H), 2.00 - 1.76 (m, 2H), 1.71 - 1.57 (m,

1H), 1.56 - 1.46 (m, 1H), 1.30 (d, J=6.4 Hz, 3H); HRMS for $C_{26}H_{28}F_3N_4O_4$ MS m/z $[M+H]^+$ Calcd 517.2057, found 517.2065.

**(R)-5-(1-methyl-1H-imidazol-4-yl)-2-((1-(2-(4-(trifluoromethoxy)phenyl)propanoyl)piperidin-4-yl)oxy)benzamide (5).** See procedures for compound **3**, then using general EDC coupling procedures **F** and appropriate carboxylic acid, then chiral separation of enantiomers: LCMS [M+1] 517.2; $^1$H NMR (400 MHz, d-DMSO) δ ppm 8.06 (dd, J = 11.08, 2.04 Hz, 1H), 7.73 (d, J = 8.64 Hz, 1H), 7.59 (s, 1H), 7.53 (bs, 2H), 7.42 (m, 3H), 7.32 (d, J = 8.32 Hz, 2H), 7.14 (d, 8.64 Hz, 1H), 4.68 (m, 1H), 4.25 (m, 1H), 3.82 (m, 2H), 3.66 (s, 3H), 3.45 (m, 1H), 3.24 (m, 1H), 1.88 (m, 2H), 1.63 (m, 1H), 1.53 (m, 1H), 1.30 (d, J = 6.76 Hz, 3H); HRMS for $C_{26}H_{28}F_3N_4O_4$ MS m/z $[M+H]^+$ Calcd 517.2057, found 517.2067.

**2-((1-(2-(3-fluoro-4-(trifluoromethoxy)phenyl)acetyl)piperidin-4-yl)oxy)-5-(1-methyl-1H-imidazol-4-yl)benzamide (6).** See procedures for compound **3**, then using general HATU coupling procedures **C** and appropriate carboxylic acid : LCMS [M+1] 521.4; $^1$H NMR (400 MHz, d-DMSO) δ ppm 8.11 (d, J=2.3 Hz, 1H), 7.77 (dd, J=2.3, 8.6 Hz, 1H), 7.74 (s, 1H), 7.60 (s, 1H), 7.54 (br. s., 2H), 7.49 (t, J=8.4 Hz, 1H), 7.37 (dd, J=1.7, 11.6 Hz, 1H), 7.22 (d, J=8.8 Hz, 1H), 7.18 (d, J=8.3 Hz, 1H), 4.85 - 4.71 (m, 1H), 3.88 - 3.73 (m, 4H), 3.69 (s, 3H), 3.50 - 3.40 (m, 1H), 3.39 - 3.35 (m, 1H), 2.01 - 1.86 (m, 2H), 1.78 - 1.54 (m, 2H); HRMS for $C_{25}H_{25}F_4N_4O_4$ m/z $[M+H]^+$ Calcd 521.1806, found 521.1813.

**2-((1-(2-(4-cyclopropoxy-3-fluorophenyl)acetyl)piperidin-4-yl)oxy)-5-(1-methyl-1H-imidazol-4-yl)benzamide (7).** See procedures for compound **3**, then using general HATU coupling procedures **C** and appropriate carboxylic acid : LCMS [M+1] 475.0; $^1$H NMR (400 MHz, d-DMSO) δ ppm 8.09 (d, J=2.3 Hz, 1H), 7.76 (dd, J=2.4, 8.6 Hz, 1H), 7.60 (s, 1H), 7.54 (d, J=1.1

Hz, 1H), 7.51 (s, 2H), 7.20 - 7.11 (m, 3H), 7.01 - 6.94 (m, 2H), 4.79 - 4.66 (m, 1H), 3.85 - 3.74 (m, 5H), 3.67 (s, 3H), 3.47 - 3.34 (m, 2H), 1.99 - 1.79 (m, 2H), 1.71 - 1.48 (m, 2H), 0.79 - 0.71 (m, 2H), 0.66 - 0.58 (m, 2H; HRMS for $C_{27}H_{31}N_4O_4$ MS m/z $[M+H]^+$ Calcd 475.234, found 475.2346.

**5-(1-methyl-1H-imidazol-4-yl)-2-((1-(2-(4-(trifluoromethoxy)phenyl)acetyl)piperidin-4-yl)oxy)nicotinamide (8)**. See procedures for **9b** using appropriate piperidine and **32**. LCMS [M+1] 504.6; $^1$H NMR (400 MHz, d-DMSO) δ ppm 8.61 (d, J = 2.4 Hz, 1H), 8.45 (d, J = 2.36 Hz, 1H), 7.73 (bs, 1H), 7.66 (s, 2H), 7.57 (bs, 1H), 7.36 (d, J = 8.6 Hz, 2H), 7.30 (d, 8.32 Hz, 2H), 5.41-5.38 (m, 1H), 3.87-3.76 (m, 4H), 3.68 (s, 3H), 3.49-3.40 (m, 2H), 2.0-1.97 (m, 2H), 1.72-1.68 (m, 2H); HRMS ESI [M+1] calc for $C_{24}H_{24}F_3N_5O_4$ 504.1853; found 504.1859.

**2-(((3R,4R)-3-fluoro-1-(2-(4-(trifluoromethoxy)phenyl)acetyl)piperidin-4-yl)oxy)-5-(1-methyl-1H-imidazol-4-yl)nicotinamide (9a)**. See procedures for **9b** using appropriate piperidine. LCMS [M+1] 521.8; $^1$H NMR (400 MHz, MeOD-$d_4$) δ ppm 8.64 (br. s., 1H), 8.52 (br. s., 1H), 7.68 (s, 1H), 7.52 (s, 1H), 7.37 (d, J=7.8 Hz, 2H), 7.24 (d, J=7.8 Hz, 2H), 5.67 - 5.51 (m, 1H), 4.80 - 4.73 (m, 2H), 4.16 - 3.82 (m, 4H), 3.78 (s, 3H), 3.65-3.60 (m, 1H), 2.23-2.19 (m, 1H), 1.96 - 1.70 (m, 1H) ; HRMS for $C_{24}H_{24}F_4N_5O_4$ MS m/z $[M+H]^+$ Calcd 522.1759; found 522.1761.

**2-(((3S,4S)-3-fluoro-1-(2-(4-(trifluoromethoxy)phenyl)acetyl)piperidin-4-yl)oxy)-5-(1-methyl-1H-imidazol-4-yl)nicotinamide (9b).** To a stirred solution of tert-butyl (3S,4S)-3-fluoro-4-hydroxypiperidine-1-carboxylate **36** (512 mg, 2.34 mmol) in DMSO (10 mL) was added t-BuOK (393 mg, 3.50 mmol) at 15 $^o$C. The resulting mixture was stirred at 15 $^o$C for 30 minutes, then 5-bromo-2-chloronicotinamide **37** (550 mg, 2.34 mmol) was added at 15 $^o$C. The resulting mixture was stirred at 15 $^o$C for 12 hours. To the mixture was added water (15 mL) and EtOAc (25 mL).

The organic layer was separated and the aqueous layer was extracted with EtOAc (10 mL x 2). The organic layers were combined, washed with water (10 mL x 3) and brine (8 mL x 2), dried over $Na_2SO_4$, filtered, and concentrated i*n vacuo* to give the crude product which was purified by Biotage ($SiO_2$, Rf =0.5 Petroleum ether/EtOAc =1:1) to obtain **38** (700 mg, 72%) as a yellow oil. LCMS [M-Boc+1] 319; $^1$H NMR (400 MHz, CDCl3) δ ppm 8.61 (d, J=2.5 Hz, 1H), 8.29 (d, J=2.5 Hz, 1H), 7.56 - 7.40 (m, 1H), 6.09 - 5.88 (m, 1H), 5.51 - 5.37 (m, 1H), 4.80- 4.55 (m, 1H), 4.36 - 4.15 (m, 1H), 3.93 - 3.83 (m, 1H), 3.18 (br s, 2H), 2.47 - 2.35 (m, 1H), 1.67 (br d, J=10.3 Hz, 1H), 1.48 (s, 9H). Using general HCl deprotection procedures **B**, compound **38** (700 mg, 1.67 mmol) deprotected to give **39** (550 mg, >99%) and used directly in the next step. LCMS [M+1] 319. Using coupling conditions using general HATU procedure **C**, Compound **39** (550 mg, 1.55 mmol) coupled with **29** to give **40** (750 mg, 93%) as a yellow oil and used directly in the next step. LCMS [M+1] 521.Using general $B_2Pin_2$ procedures **D**, Compound **40** (750 mg, 1.44 mmol) afforded **41** (500 mg, 61%) as a brown oil and used directly in the next step. LCMS [M-pinacol+1] 486. To a mixture of **41** (500 mg, 0.88 mmol), **42** (367 mg, 1.76 mmol), $K_2CO_3$ (487 mg, 3.53 mmol) in DMF (15 mL) and water (3 mL) was added Pd(dppf)$Cl_2$ (64.5 mg, 0.088 mmol) at 20 $^oC$ under $N_2$ atmosphere. The resulting mixture was purged with $N_2$ three times and heated at 100 $^oC$ for 12 hours. To the mixture was added EtOAc (25 mL) and water (10 mL). The organic layer was separated and the aqueous layer was extracted with EtOAc (25 mL x 3). The combined organic layers were washed with water (15 mL x 3) and brine (15 mL x 2), dried over $Na_2SO_4$, filtered and concentrated *in vacuo* to give the crude product, which was purified by prep. TLC (Rf =0.4 in DCM/MeOH =10:1) to obtain the desired product **9b** (110 mg, 24%) as an off-white solid. LCMS [M+1] 521.9; HRMS for $C_{24}H_{23}F_4N_5O_4$ MS m/z [M] Calcd 521.1686; found 521.1694; $^1$H NMR (400 MHz, d-DMSO) δ ppm 8.63 (d, J=2.4 Hz, 1H), 8.46 (t, J=2.8 Hz, 1H), 7.74 (d, J=8.9 Hz,

1H), 7.69 (br. s, 1H), 7.67 (s, 1H), 7.60 (br. s., 1H), 7.36 (d, J=10.4 Hz, 2H), 7.30 (d, J=8.3 Hz, 2H), 5.58 - 5.43 (m, 1H), 5.06 - 4.74 (m, 1H), 4.12 - 3.93 (m, 1H), 3.91 - 3.71 (m, 3H), 3.68 - 3.59 (m, 1H), 3.58 - 3.38 (m, 1H), 2.16 - 2.01 (m, 1H), 1.89 - 1.67 (m, 1H).

**2-(((3S,4R)-3-fluoro-1-(2-(4-(trifluoromethoxy)phenyl)acetyl)piperidin-4-yl)oxy)-5-(1-methyl-1H-imidazol-4-yl)nicotinamide (10a)**. See procedures for **9b** using appropriate piperidine. LCMS [M+1] 522.0; $^{1}$H NMR (400 MHz, d-DMSO) δ ppm 8.64 (d, J = 2.2 Hz, 1H), 8.54 (d, J = 2.2 Hz, 1H), 7.83 (bs, 1H), 7.70 (s, 1H), 7.67 (s, 1H), 7.53 (bs, 1H), 7.36-2.29 (m, 4H), 5.56-5.49 (m, 1H), 5.18-5.03 (m, 1H), 4.63-4.34 (m, 2H), 4.03-3.83 (m, 2H), 3.73-3.63 (m, 4H), 3.25-2.91 (m, 1H), 2.02-1.98 (m, 1H), 1.90-1.76 (m, 1H).

**2-(((3R,4S)-3-fluoro-1-(2-(4-(trifluoromethoxy)phenyl)acetyl)piperidin-4-yl)oxy)-5-(1-methyl-1H-imidazol-4-yl)nicotinamide (10b)**. See procedures for **9b** using appropriate piperidine. LCMS [M+1] 522.28; $^{1}$H NMR (400 MHz, d-DMSO) δ ppm 8.65 (t, J=2.5 Hz, 1H), 8.55 (t, J=2.4 Hz, 1H), 7.83 (br. s., 1H), 7.71 (s, 1H), 7.69 (s, 1H), 7.54 (br. s., 1H), 7.41 - 7.25 (m, 4H), 5.67 - 5.41 (m, 1H), 5.23 - 4.95 (m, 0.5H), 4.67 - 4.34 (m, 1H), 4.33 - 3.98 (m, 0.5H), 3.92 - 3.73 (m, 2H), 3.70 (s, 3H), 3.68 - 3.52 (m, 1H), 3.29 - 2.90 (m, 1H), 2.09 - 1.99 (m, 1H), 1.92 - 1.72 (m, 1H); $^{19}$F NMR (376 MHz, d6-DMSO): δ -57; HRMS for $C_{24}H_{24}F_4N_5O_4$ MS m/z $[M+H]^+$ Calcd 522.1759; found 522.1767.

**2-((3,3-difluoro-1-(2-(4-(trifluoromethoxy)phenyl)acetyl)piperidin-4-yl)oxy)-5-(1-methyl-1H-imidazol-4-yl)benzamide (11)**. Tert-butyl 3,3-difluoro-4-hydroxypiperidine-1-carboxylate **43** (155 mg, 0.66 mmol), 5-bromo-2-fluorobenzamide **44** (140 mg, 0.64 mmol) and $Cs_2CO_3$ (314 mg, 0.96 mmol) were suspended in DMF (3.2 mL) in a 25 mL round bottom flask and heated at 105 $^{o}$C for 25 hours. The reaction was reduced to near dryness under vacuum and the residue was

dissolved in water (30 mL) and EtOAc (20 mL). The EtOAc layer was extracted and the aqueous was back-extracted with EtOAc (2 x 10 mL). The organics were combined with the crude material from a previous experiment run in a similar manner (0.1 mmol scale in 5-bromo-2-fluorobenzamide), washed with 20% brine solution (2 x 5 mL), dried over $Na_2SO_4$, filtered and the filtrate was concentrated to dryness under vacuum. The residue was purified by $SiO_2$ chromatography, eluting with an EtOAc/heptane gradient, to obtain **45** (0.294 g, 90%) as an off-white solid. LCMS [M-Boc+1] 335.2; $^1$H NMR (600 MHz, $CDCl_3$) δ ppm 8.29 (br. s., 1H), 7.56 (d, J=8.8 Hz, 1H), 7.34 (br. s., 1H), 6.89 (d, J=8.8 Hz, 1H), 5.83 (br. s., 1H), 4.53 - 4.70 (m, 1H), 4.11 (br. s., 1H), 3.83 (br. s., 1H), 3.49 - 3.62 (m, 1 H), 3.32 (t, J=10.9 Hz, 1H), 2.16 (br. s., 1H), 2.03 (br. s., 1H), 1.49 (s, 9H). Using similar conditions as general $B_2Pin_2$ procedures **D** to obtain **46** and used directly in the next step. Using similar conditions as general Suzuki procedures **E** to obtain **47** (74 mg, 25%) as a tan foam. LCMS [M+1] 437.4; $^1$H NMR (600 MHz, $CDCl_3$) δ ppm 8.38 (s, 1H), 8.04 (d, J=8.8 Hz, 1H), 7.43 - 7.51 (m, 2H), 7.25 (s, 1H), 7.03 (d, J=8.8 Hz, 1H), 5.78 (br. s., 1H), 4.61 - 4.75 (m, 1H), 4.11 (br. s., 1H), 3.82 (br. s, 1H), 3.73 (s, 3H), 3.53 - 3.66 (m, 1H), 3.35 (t, J=10.3 Hz, 1H), 2.18 (br. s., 1H), 2.05 (br. s, 1H), 1.49 (s, 9H). Using similar conditions as general HCl deprotection procedures **B** to obtain **48** and used crude directly in the next step. Compound **48** (67.5 mg, 0.165 mmol) and **29** (60 mg, 0.27 mmol) were suspended in DMF (1.25 mL) and to the brown mixture was added DIEA (0.16 mL, 0.92 mmol) leading to a dark brown solution. COMU (107 mg, 0.24 mmol) was added as a solid in one portion and the reaction was stirred at room temperature for 14 hours. The reaction was reduced to near dryness under vacuum and the dark residue was diluted with saturated sodium bicarbonate (20 mL) and EtOAc (20 mL). The organic layer was extracted and the aqueous was back-extracted with EtOAc (10 mL). The organics were combined, washed with saturated brine, dried over $Na_2SO_4$, filtered

and the filtrate was concentrated under vacuum. The isolate was purified by $SiO_2$ chromatography, eluting with 0-8% MeOH/DCM to obtain compound **11** (72 mg, 81% yield) a light brown solid. LCMS [M+1] 539.4; $^1$H NMR (600 MHz, DMSO-$d_6$) δ ppm 8.06 (s, 1H), 7.79 (d, J=8.8 Hz, 1H), 7.63 (s, 1H), 7.59 (s, 2H), 7.48 (br. s., 1H), 7.33 - 7.39 (m, 2H), 7.29 - 7.33 (m, 2H), 7.27 (d, J=8.80 Hz, 1H), 5.14-5.05 (m, 1H), 4.15 - 4.32 (m, 1H), 3.71 - 3.99 (m, 4H), 3.68 (s, 3H), 3.36 - 3.59 (m, 1H), 2.10-2.02 (m, 1H), 1.72 - 1.90 (m, 1H).

**2-(((3R,4R)-3-fluoro-1-(2-(4-(trifluoromethoxy)phenyl)acetyl)piperidin-4-yl)oxy)-4-(2-hydroxy-2-methylpropoxy)benzamide (12a).** See procedures for **13b** with the appropriate piperidine (30 mg, 52%): LCMS [M+1] 529.2; $^1$H NMR (400 MHz, DMSO-$d_6$) δ ppm 7.77 (d, J=8.3 Hz, 1H), 7.44 - 7.25 (m, 5H), 6.78 (s, 1H), 6.65 (d, J=8.8 Hz, 1H), 5.00 - 4.70 (m, 2H), 4.65 (s, 1H), 4.28 - 4.06 (m, 1H), 3.98 - 3.71 (m, 4H), 3.62 - 3.36 (m, 2H), 3.27 - 3.18 (m, 1H), 2.13 - 1.98 (m, 1H), 1.82 - 1.57 (m, 1H), 1.20 (s, 6H).

**2-(((3S,4S)-3-fluoro-1-(2-(4-(trifluoromethoxy)phenyl)acetyl)piperidin-4-yl)oxy)-4-(2-hydroxy-2-methylpropoxy)benzamide (12b)**. See procedures for **13b** with the appropriate piperidine (30 mg, 26%): LCMS [M+1] 529.2; $^1$H NMR (400 MHz, DMSO-$d_6$) δ ppm 7.77 (d, J=8.8 Hz, 1H), 7.47 - 7.24 (m, 5H), 6.78 (d, J=2.0 Hz, 1H), 6.65 (dd, J=2.0, 8.8 Hz, 1H), 4.99 - 4.70 (m, 2H), 4.65 (s, 1H), 4.25 - 4.04 (m, 1H), 3.94 - 3.72 (m, 4H), 3.62 - 3.38 (m, 2H), 3.28 - 3.17 (m, 1H), 2.12 - 1.98 (m, 1H), 1.78 - 1.58 (m, 1H), 1.22 (s, 6H).

**2-(((3S,4R)-3-fluoro-1-(2-(4-(trifluoromethoxy)phenyl)acetyl)piperidin-4-yl)oxy)-4-(2-hydroxy-2-methylpropoxy)benzamide (13a)**. See procedures for **13b** with the appropriate piperidine (35 mg, 38%): LCMS [M+1] 529.2; $^1$H NMR (400 MHz, DMSO-$d_6$) δ ppm 7.88 (d, J=8.8 Hz, 1H), 7.43 (d, J=15.7 Hz, 2H), 7.37 - 7.23 (m, 4H), 6.81 (br. s., 1H), 6.68 (d, J=8.8 Hz,

1H), 5.17 - 4.95 (m, 2H), 4.65 (s, 1H), 4.42 - 4.28 (m, 1H), 4.01 (d, J=12.7 Hz, 1H), 3.90 - 3.65 (m, 4H), 3.58 - 3.40 (m, 1H), 3.14 - 2.83 (m, 1H), 2.01 - 1.88 (m, 1H), 1.79 - 1.61 (m, 1H), 1.21 (s, 6H).

**2-(((3R,4S)-3-fluoro-1-(2-(4-(trifluoromethoxy)phenyl)acetyl)piperidin-4-yl)oxy)-4-(2-hydroxy-2-methylpropoxy)benzamide (13b).** A solution of 4-(benzyloxy)-2-fluorobenzonitrile **49** (1.0 g, 4.401 mmol), tert-butyl (3R,4S)-3-fluoro-4-hydroxypiperidine-1-carboxylate **50** (1.065 g, 4.841 mmol) and $Cs_2CO_3$ (2.86 g, 8.802 mmol) in DMF (20 mL) was heated at 100 °C for 16 hours in a sealed tube. The reaction mixture was diluted with EtOAc and washed with water and brine, dried over $Na_2SO_4$ and concentrated. The crude was purified by column chromatography ($SiO_2$, 10% EtOAc in hexane) to afford **51** (1.7 g, 90.4%) as a yellow gum. LCMS [M+1] 427.1; $^1$H NMR (400 MHz, d-DMSO) δ ppm 7.66 (d, J = 8.64 Hz, 1H), 7.47-7.35 (m, 5H), 6.99 (s, 1H), 6.78 (dd J = 8.56 Hz, 1H), 5.20 (s, 2H), 4.98-4.86 (m, 3H),4.05-4.03 (m, 2H), 3.84-3.80 (m, 1H), 1.82-1.80 (m, 2H), 1.40 (s, 9H). Using similar conditions as general hydrolysis procedures **A** to obtain **52** (900 mg, 51%). LCMS [M+1] 445.3. Using similar conditions as general HCl deprotection procedures **B** to obtain **53** (695 mg, > 99%) and used directly in the next step. LCMS [M+1] 345.2. Using similar conditions as general EDCI coupling procedures **F** to obtain **54** (900 mg, 82%). LCMS [M+1] 547.1. A solution of compound **54** (900 mg, 1.648 mmol) in EtOH (25 ml) was degassed with argon for about 10 min followed by the addition of Pd/C (400 mg). The resultant mixture was then stirred under $H_2$ atmosphere (balloon pressure) for 2 hours at ambient temperature. The reaction mixture was then filtered through a pad of celite which was further washed with MeOH. The filtrate was evaporated to dryness *in vacuo* to afford **55** (700 mg, 93%) of as a white solid. LCMS [M+1] 456.9. To a solution of compound **55** (500 mg, 1.096 mmol) in DMF (8 mL) in a sealed tube were added $K_2CO_3$ (302 mg, 2.193 mmol) and isobutylene oxide

(0.489 mL, 5.482 mmol). The cap was tightened and the reaction mixture was heated at 100 °C for 16 hours. The reaction mixture was brought to room temperature and was diluted with EtOAc. The organic layer was washed with water, brine, dried over $Na_2SO_4$ and concentrated under reduced pressure. The crude was purified by Combiflash column (5-7% MeOH in DCM) to give **13b** (150 mg, 26%). LCMS [M+1] 529.3; $^1$H NMR (600 MHz, DMSO-$d_6$) δ ppm 7.89 (dd, J=1.5, 8.8 Hz, 1H), 7.46 (br. s., 1H), 7.41 (br. s., 1H), 7.38 - 7.34 (m, 2H), 7.33 - 7.26 (m, 2H), 6.83 - 6.77 (m, 1H), 6.68 (d, J=8.8 Hz, 1H), 5.18 - 5.04 (m, 1H), 5.03 - 4.95 (m, 1H), 4.73 - 4.62 (m, 1H), 4.45 - 4.28 (m, 1H), 4.08 - 3.88 (m, 1H), 3.85 (s, 1H), 3.79 (s, 2H), 3.74 - 3.40 (m, 1H), 3.32 - 3.21 (m, 1H), 3.17 - 2.80 (m, 1H), 2.05 - 1.89 (m, 1H), 1.81 - 1.60 (m, 1H), 1.22 (s, 6H); HRMS for $C_{25}H_{28}F_4N_2O_6$ MS m/z [M] Calcd 528.1883; found 528.1892.

**2-(((3S,4R)-3-fluoro-1-(2-(4-(trifluoromethoxy)phenyl)acetyl)piperidin-4-yl)oxy)-4-((1-hydroxy-2-methylpropan-2-yl)oxy)benzamide (14)**. To a stirred solution of compound **56** (see procedures **13b** using the appropriate piperidine, 100 mg, 0.219 mmol) in DMF (5 mL) was added 2-bromo-2-methyl propionic acid methyl ester (0.043 mL, 0.329 mmol) and $Cs_2CO_3$ (142.5 mg, 0.439 mmol) at room temperature. The reaction was heated to 100-110°C for 16 hours in a sealed tube. The reaction was diluted with EtOAc and the organic layer was washed with water, brine and dried over $Na_2SO_4$. The solution was then evaporated to obtain the crude compound which was purified through a column using 100-200 $SiO_2$ with 2% MeOH/DCM to afford **57** (120 mg, 98%) as an off white colored sticky compound and used directly in the next step. To a stirred solution of compound **57** (50 mg, 0.09 mmol) in THF-water (5 mL:1 mL), LiOH (15.1 mg, 0.36 mmol) was added and the mixture stirred for 4 hours at room temperature. The reaction mass was acidified by 1N HCl (pH 3-4) and extracted with EtOAc. The organic solution was dried over $Na_2SO_4$ and evaporated to obtain compound **58** (40 mg, 82%) as a light green solid. The next step

was performed with this material without any purification. LCMS [M+1] 543.6. To a solution of compound **58** (40 mg, 0.074 mmol) in THF (5.0 mL) at 0°C, TEA (0.021 mL, 0.148 mmol) and isobutyl chloroformate (0.015 mL, 0.111 mmol) were added at 0°C under $N_2$. The reaction was allowed to warm to room temperature and stirred for 2 hours. The reaction mixture was then filtered through celite under $N_2$. $NaBH_4$ solution (5.6 mg dissolved in 2 mL water) was then added and the reaction mixture stirred for another 1 hour and then diluted with EtOAc. The organic layer was washed with water, brine, dried over $Na_2SO_4$ and evaporated to obtain the crude material which was purified by preparative TLC using 3% MeOH/DCM to afford **14** (20 mg, 51%) as an off white colored solid. LCMS [M+1] 529.4; $^1$H NMR (400 MHz, DMSO-$d_6$) δ ppm 7.82 (J = 8.6 Hz, 1H), 7.50 (bs, 1H), 7.43 (bs, 1H), 7.35 (d, J = 8.6 Hz, 2H), 7.29 (d, J = 8.04 Hz, 2H), 6.85 (s, 1H), 6.76 (d, J = 8.64 Hz, 1H), 5.2-4.95 (m, 3H), 4.75-1.33 (m, 1H), 4.10-3.83 (m, 2H), 3.71-3.30 (m, 1H), 3.42 (d, J = 5.72 Hz, 2H), 3.25-2.90 (m, 1H), 1.95-1.93 (m, 1H), 1.85-1.75 (m, 1H), 1.27 (s, 6H).

**1-(4-((2-amino-5-(1-methyl-1H-pyrazol-4-yl)pyridin-3-yl)oxy)piperidin-1-yl)-2-(4-(trifluoromethoxy)phenyl)ethan-1-one (15).** See procedures step 1-4 for compound **16b**, but different coupling using T3P. To a solution of **63** (50 mg, 0.183 mmol), compound **29** (40 mg, 0.183 mmol) TEA (0.080 mL, 0.40 mmol) in THF (15 mL) was added T3P (0.27 mL, 0.457 mmol). The reaction was stirred at room temperature for 16 hours, then concentrated and diluted with water and DCM. The DCM layer was washed with $NaHCO_3$ (sat aq) and concentrated. The crude material was purified by prep HPLC to obtain **15** (18 mg, 21%). LCMS [M+1] 476.2; $^1$H NMR (400 MHz, DMSO-$d_6$) δ ppm 7.96 (s, 1H), 7.73 (s, 2H), 7.35 (d, J = 8.68 Hz, 2H), 7.29-7.26 (m, 3H), 4.68-4.65 (m, 1H), 3.81 (s, 3H), 3.77 (s, 2H), 3.66-3.60 (m, 2H), 3.44-3.42 (m, 2H), 1.85-1.82 (m, 2H), 1.60-1.57 (m, 2H).

**(S)-1-(3-((2-amino-5-(1-methyl-1H-pyrazol-4-yl)pyridin-3-yl)oxy)pyrrolidin-1-yl)-2-(4-(trifluoromethoxy)phenyl)ethan-1-one (16a).** See procedures for **16b** to obtain **16a** (21 mg, 30%). LCMS [M+1] 462.2. $^1$H NMR (400 MHz, DMSO-$d_6$) δ ppm 8.00 (d, J=3.1 Hz, 1H), 7.79 (d, J=1.3 Hz, 1H), 7.76 (s, 1H), 7.39 - 7.21 (m, 5H), 5.64 (d, J=8.9 Hz, 2H), 5.20 - 5.03 (m, 1H), 3.83 (d, J=2.1 Hz, 3H), 3.79 - 3.65 (m, 4H), 3.61 - 3.47 (m, 2H), 2.25 - 2.17 (m, J=4.0 Hz, 1H), 2.15 - 2.05 (m, J=2.0 Hz, 1H); HRMS for $C_{22}H_{23}F_3N_5O_3$ MS m/z $[M+H]^+$ Calcd: 462.1748; found 462.1752.

**(R)-1-(3-((2-amino-5-(1-methyl-1H-pyrazol-4-yl)pyridin-3-yl)oxy)pyrrolidin-1-yl)-2-(4-(trifluoromethoxy)phenyl)ethan-1-one (16b).** To a degassed mixture of 1-methyl-4-(4,4,5,5-tetramethyl-1,3,2-dioxaborolan-2-yl)-1H-pyrazole (27.5 g, 132 mmol), 6-bromooxazolo[4,5-b]pyridin-2(3H)-one **59**,[49,50] (23.65g, 110 mmol), $Na_2CO_3$ (37.7 g, 356 mmol), water (117 mL) and 1,4-dioxane (186 mL), was added $PdCl_2$(dppf) (6.46 g, 8.83 mmol) and the mixture heated at 90 °C under argon for 18 hours. The reaction mixture was cooled to ambient temperature and concentrated under reduced pressure. The residue was suspended in HCl solution (2 L, 1N aqueous), stirred at ambient temperature for 1 hour and the solids collected by vacuum filtration to afford **60**,[49-50] as a purple/beige solid (21.4 g, 90%). UPLC [M+1] 217.08; $^1$H NMR (300 MHz, DMSO-$d_6$) δ ppm 8.28 (s, 1H), 8.16 (s, 1H), 7.90 (s, 1H), 7.85 (s, 1H), 3.83 (s, 3H). To a suspension of **60** (21.4 g, 99.1 mmol) in MeOH (215 mL), was added a solution of NaOH (25.7 g, 643 mmol) in water (215 mL) and the mixture heated at reflux for 18 hours. The reaction mixture was cooled to ambient temperature and concentrated under reduced pressure to remove the MeOH. The remaining aqueous phase was adjusted to pH 12 with NaOH, diluted with MeOH (215 mL) and heated at reflux for a further 18 hours. The reaction mixture was cooled to ambient temperature, adjusted to pH 6 with HCl (6N aqueous) and concentrated under reduced pressure.

The residue was triturated in 9:1 DCM:MeOH (2 x 70 mL), filtered under vacuum and the filtrate concentrated under reduced pressure. The crude material was purified by $SiO_2$ column chromatography, eluting with MeOH:DCM first, then $NH_3$/MeOH (18% ammonia basis) to afford **61** as a dark green/brown foam (13.5 g, 72%). UPLC [M+1] 190.98; $^1$H NMR (300 MHz, DMSO-$d_6$) δ ppm 7.86 (s, 1H), 7.63 (s, 1H), 7.60 (s, 1H), 6.93 (s, 1H), 5.38 (bs, 2H), 3.80 (s, 3H). To a mixture of **61** (13.3 g, 69.6 mmol), (S)-tert-butyl 3-((methylsulfonyl)oxy)pyrrolidine-1-carboxylate (22.5 g, 84.8 mmol) and DMF (150 mL), was added $Cs_2CO_3$ (34.3 g, 105 mmol) and the mixture heated at 85 °C for 8 hours. The reaction mixture was cooled to ambient temperature, poured onto water (1.5 L), diluted with EtOAc (500 mL) and filtered under vacuum. The filtrate layers were separated and the aqueous layer was extracted into EtOAc (3 x 500 mL). The combined organic extracts were washed with brine (500 mL), dried over $MgSO_4$, filtered and the solvent removed under reduced pressure. The crude material was purified by $SiO_2$ column chromatography, eluting with 10% MeOH/EtOAc to afford **62** (13.0 g, 52%). UPLC [M+1] 360.26; $^1$H NMR (300 MHz, DMSO-$d_6$) δ ppm 7.99 (s, 1H), 7.75 (s, 1H), 7.73 (s, 1H), 7.18 (s, 1H), 5.61 (bs, 2H), 4.98-5.02 (m, 1H), 3.80 (s, 3H), 3.60-3.30 (m, 4H), 2.10-2.00 (m, 2H), 1.37 (s, 9H). See general HCl deprotection procedures **B** using **62** (13 g, 36.2 mmol) to afford **63** as the HCl salt (12.7 g, >99%). LCMS [M+1] 260.05; $^1$H NMR (300 MHz, DMSO-$d_6$) δ ppm 9.88 (bs, 1H), 9.52 (bs, 1H), 8.22 (s, 1H), 8.09 (bs, 2H), 7.93 (s, 1H), 7.76 (d, J = 4.59 Hz, 2H), 5.48-5.45 (m, 1H), 3.84 (s, 3H), 3.53-3.25 (m, 4H), 2.21-2.12 (m, 2H). Using general HATU coupling procedures **C** with **63** (12.3 g, 41.5 mmol) afforded **16b** as a brown foam (11.4 g, 73%). LCMS [M+1] 461.92; $^1$H NMR (400 MHz, DMSO-$d_6$) δ ppm 8.00 (d, J=3.1 Hz, 1H), 7.79 (d, J=1.3 Hz, 1H), 7.76 (s, 1H), 7.40 - 7.29 (m, 3H), 7.29 - 7.21 (m, 2H), 5.65 (s, 1H), 5.63 (s, 1H), 5.19 - 5.04 (m, 1H), 3.90 - 3.84 (m, 1H), 3.83 (d, J=2.1 Hz, 3H), 3.78 - 3.67 (m, 3H), 3.62 - 3.47 (m, 2H), 2.25

- 2.18 (m, 1H), 2.14 - 2.06 (m, 1H) ; $^{19}$F NMR (DMSO-$d_6$, 283 MHz) δ ppm -56.70; HRMS for $C_{22}H_{22}F_3N_5O_3$ MS m/z [M] calcd 461.1675; found 461.1661.

**1-((3S,4S)-3-((2-amino-5-(1-methyl-1H-imidazol-4-yl)pyridin-3-yl)oxy)-4-fluoropyrrolidin-1-yl)-2-(4-(trifluoromethoxy)phenyl)ethan-1-one (17a) and 1-((3R,4R)-3-((2-amino-5-(1-methyl-1H-imidazol-4-yl)pyridin-3-yl)oxy)-4-fluoropyrrolidin-1-yl)-2-(4-(trifluoromethoxy)phenyl)ethan-1-one (17b).** A suspension of 6-oxa-3-aza-bicyclo[3.1.0]hexane-3- carboxylic acid benzyl ester **64** (1.1g, 5 mmol) in HF.TEA (0.8 mL) was heated to 115 °C in a microwave reactor for 45 min. The reaction mixture was poured into cold saturated $NaHCO_3$ then extracted with EtOAc. The EtOAc layer was washed with brine, dried with $Na_2SO_4$, filtered then concentrated to an oil. The crude mixture was purified by $SiO_2$ chromatography (ISCO-Rf-24g column) eluting with a gradient of 0-100% EtOAc-heptane to afford ±**65** (974 mg, 81%) as a colorless oil. LCMS-ESI(+) [M+1] 240; $^1$H NMR (400 MHz, $CDCl_3$) δ ppm 7.42 - 7.29 (m, 5H), 5.16 (s, 2H), 5.07 - 4.83 (m, 1H), 4.42 (d, J=3.2 Hz, 1H), 3.87 - 3.50 (m, 4H). To a solution of $PPh_3$ (1.98 g, 7.56 mmol) in THF (21 mL) was added DIAD (1.5 mL, 7.56 mmol). A white precipitate slowly formed. After 60 minutes a solution of ±**65** (1.51 g, 6.3 mmol) and p-nitrobenzoic acid (1.05 g, 6.3 mmol) in THF (5 mL) was added. The reaction mixture was stirred at room temperature for 67 hours then quenched with saturated $NaHCO_3$ . The quenched reaction was stirred for 10 minutes. The mixture was then diluted with water and EtOAc. The EtOAc layer was washed with brine, dried with $Na_2SO_4$, filtered and concentrated to an oil. The crude reaction mixture was purified by $SiO_2$ chromatography (ISCO-Rf-40g column) eluting with 0-50% EtOAc-heptane to obtain ±**66**. The material was used directly in the next step. LCMS [M+Na] 411. A mixture of ±**66** (2.74g) and 1N NaOH (21 mL) in MeOH (30 ml) was stirred at room temperature for 18 hours. The reaction mixture was concentrated to remove MeOH and then

partitioned between water and EtOAc. The EtOAc layer was washed with brine, dried with $Na_2SO_4$, filtered and concentrated to an oil. The crude reaction mixture was purified by $SiO_2$ chromatography (ISCO-Rf-24g column) eluting with a gradient of 0-50% EtOAc-heptane to obtain ±**67** (860 mg, 57% over 2 steps) as a colorless oil. LCMS-ESI(+) [M+Na] 262; $^1$H NMR (400 MHz, $CDCl_3$) δ ppm 7.43 - 7.29 (m, 5H), 5.15 (s, 2H), 5.11 - 4.92 (m, 1H), 4.40 - 4.25 (m, 1H), 3.92 - 3.56 (m, 3H), 3.40 - 3.21 (m, 1H). To a solution of ± **67** (860 mg, 1.25 mmol) in DCM (30 mL) cooled in an ice-water bath was added pyridine (1.7 mL) followed by the drop-wise addition of triflic anhydride (1.5 mL, 1.3 equiv.) and the mixture stirred for 45 minutes. The reaction mixture was quenched with cold citrate buffer (0.5 M, pH 4.5). The DCM layer was washed with brine, dried with $Na_2SO_4$, filtered then concentrated to an oil. The crude mixture was purified by $SiO_2$ chromatography (ISCO-Rf-40g Interchim column) eluting with a gradient of 0-100% EtOAc-heptane to afford ±**68** (1.2 g, 91%) as a colorless oil. LCMS-APCI(+) [M+1] 372, $^1$H NMR (400 MHz, $CDCl_3$) δ ppm 7.38 (s, 5H), 5.43 - 4.83 (m, 4H), 3.98 (dd, J=6.6, 12.0 Hz, 1H), 3.90 - 3.66 (m, 3H). A solution of 3-(benzyloxy)-5-(4,4,5,5-tetramethyl-1,3,2-dioxaborolan-2-yl)pyridin-2-amine **69**,[49] (50 g, 153 mmol), **42** (26.6 g, 128 mmol), DIPEA (111 mL, 639 mmol) in Industrial Methylated Spirits (750 mL), and water (30 mL) was degassed by bubbling $N_2$ for 1 hour. Pd(dppf)$Cl_2$-DCM (5.22 g, 63.9 mmol) was added at once and $N_2$ was bubbled through the reaction mixture for 15 minutes. The reaction mixture was stirred at 80°C for 24 hours. The reaction mixture was cooled down and evaporated. The crude was re-dissolved in DCM (250 mL) and washed with water (250 mL). The organic layer was separated and the water layer was extracted with DCM (2x 250 mL). The organics were combined and evaporated and purified by $SiO_2$ chromatography eluting 10-15% MeOH/EtOAc to obtain the compound **70**,[49] (24.6 g, 69%) as a black solid. LCMS [M+H] 281.12; $^1$H NMR (400 MHz, DMSO-$d_6$) δ ppm 7.91 (s, 1H), 7.58 (s, 1H), 7.50-7.52 (m,

2H), 7.30-7.42 (m, 5H), 5.68 (bs, 2H), 5.15 (s, 2H), 3.65 (s, 3H). Compound **70** (68 g, 243 mmol) was dissolved in EtOH (2.5 L). 10% $Pd(OH)_2$ on carbon (17 g, 12 mmol) was added and the reaction mixture was hydrogenated at 35°C, 4 atm of $H_2$ for 48 hours. The reaction slurry was filtered over celite. Product had low solubility so the celite pad was thoroughly washed with MeOH:water 1:1 (~6 L) until washings were colorless. Organics were evaporated to dryness to afford **71** (40.45 g, 88%) as black solid. LCMS [M+1] 191; $^1$H NMR (400 MHz, DMSO-$d_6$) δ ppm 9.44 (bs, 1H), 7.80 (s, 1H), 7.53 (s, 1H), 7.31 (s, 1H), 7.20 (s, 1H), 5.38 (bs, 2H), 3.63 (s, 3H). A mixture of **71** (256 mg, 1.35 mmol), ±**68** (500 mg, 1.35 mmol) and $Cs_2CO_3$ (570 mg, 1.75 mmol) in DMF (4.49 mL) was stirred at room temperature for 18 hours. The reaction mixture was diluted with water and EtOAc and the EtOAc layer was washed with brine, dried with $Na_2SO_4$, filtered then concentrated and purified using $SiO_2$ chromatography (ISCO-Rf-12g column) eluting with a gradient of 0-50% MeOH-EtOAc to obtain ±**72** (348 mg, 63%) as a dark brown oil. LCMS-ESI(+) [M+1] 412; $^1$H NMR (400 MHz, MeOD-$d_4$) δ ppm 7.95 (s, 1H), 7.62 (s, 1H), 7.51 (d, J=7.6 Hz, 1H), 7.44 - 7.24 (m, 6H), 5.41 - 5.22 (m, 1H, CHF), 5.19 - 5.08 (m, 3H), 4.01 - 3.76 (m, 4H), 3.75 (s, 3H). To a solution of ±**72** (348 mg, 0. 841mmol) in DCM (2.8 mL) was added 33% HBr in AcOH (738 uL). The reaction mixture was stirred at room temperature for 26 hours and then concentrated to a tan solid. The solid was suspended in MTBE, sonicated and filtered to obtain ±**73** (399 mg, >99%). LCMS-ESI(+) [M+1] 278; $^1$H NMR (400 MHz, MeOD-$d_4$) δ ppm 8.98 (s, 1H), 8.07 (s, 1H), 7.97 (d, J=1.5 Hz, 1H), 7.94 (s, 1H), 5.73 - 5.51 (m, 2H), 4.10 - 4.02 (m, 1H), 4.00 (s, 3H), 3.97 - 3.74 (m, 4H). Using general HATU procedures **C** with ±**73** (65.9 mg, 0.15 mmol) and **29** (33 mg, 0.15 mmol) to afford ±**17** (50 mg, 70%) as a glass. The enantiomers were separated by chiral SFC to give **17a** as a white solid (16.25 mg, 22%) ~99% ee (-); LCMS-ESI(+) [M+H] 480; HRMS [M] calc for $C_{22}H_{22}F_4N_5O_3$ 479.1581; 479.1586; $^1$H NMR (400 MHz,

DMSO-$d_6$) δ ppm 8.01 (d, J=1.5 Hz, 1H), 7.58 (s, 1H), 7.46 (s, 2H), 7.42 - 7.23 (m, 4H), 5.74 (d, J=8.8 Hz, 2H), 5.51 - 5.25 (m, 1H), 5.24 - 5.08 (m, 1H), 4.23 - 3.69 (m, 6H), 3.67 (d, J=1.5 Hz, 3H) and **17b** as a white solid (16 mg, 22%) >99% ee (+); LCMS-ESI(+) [M+1] 480; HRMS for $C_{22}H_{22}F_4N_5O_3$ MS m/z $[M+H]^+$ Calcd 480.1653; 480.1655; $^1$H NMR (400 MHz, DMSO-$d_6$) δ ppm 8.00 (d, J=1.5 Hz, 1H), 7.56 (s, 1H), 7.45 (s, 2H), 7.40 - 7.18 (m, 4H), 5.73 (d, J=8.8 Hz, 2H), 5.54 - 5.01 (m, 2H), 4.22 - 3.68 (m, 6H), 3.66 (d, J=1.2 Hz, 3H).

**(R)-1-(4-((2-amino-5-(1-methyl-1H-imidazol-4-yl)pyridin-3-yl)oxy)-3,3-difluoropyrrolidin-1-yl)-2-(4-(trifluoromethoxy)phenyl)ethan-1-one (18a) and (S)-1-(4-((2-amino-5-(1-methyl-1H-imidazol-4-yl)pyridin-3-yl)oxy)-3,3-difluoropyrrolidin-1-yl)-2-(4-(trifluoromethoxy)phenyl)ethan-1-one (18b).** Compound **74** (540 mg, 2.42 mmol), 3-fluoro-2-nitropyridine **75** (361 mg, 2.54 mmol) and $Cs_2CO_3$ (1.58 g, 4.84 mmol) in THF (12.1 mL, 0.2 M) was heated to reflux overnight. The solvent was evaporated, water added, and the mixture extracted with EtOAc. The solvent was removed and the residue was purified by column chromatography with 35% EtOAc/heptane to give **76** (760 mg, 91% yield) as a light yellow oil. LCMS [M+$H_2O$] 363.10; $^1$H NMR (400 MHz, $CDCl_3$) δ ppm 8.23 (d, J=3.91 Hz, 1H), 7.55 - 7.69 (m, 2H), 4.85 (br. s., 1H), 3.70 - 3.99 (m, 4H), 1.50 (s, 9H). A mixture of compound **76** (760 mg, 2.20 mmol) and Pd/C (5% wet, 234 mg, 2.20 mmol) in MeOH (22.0 mL, 0.1 M) was degassed and purged with $H_2$, and stirred at room temperature under a $H_2$ balloon for 4 hours. The Pd/C was filtered and the solvent was removed to give **77** (700 mg, >99%) as a light yellow oil which was used without further purification. LCMS [M+1] 316.10. $^1$H NMR (400 MHz, $CDCl_3$) δ ppm 7.78 (d, J=5.50 Hz, 1H), 7.00 (d, J=6.97 Hz, 1H), 6.63 (dd, J=7.89, 5.07 Hz, 1H), 4.67 (br. s., 3H), 3.62 - 3.94 (m., 4H) 1.49 (s, 9H). To a mixture of compound **77** (1.29 g, 4.08 mmol) in DMF (81.6 mL, 0.05 M) was added NBS (918 mg, 4.90 mmol) portion-wise, and the whole stirred at room temperature for

5 min after which water and EtOAc were added. The layers were separated, the organic layer was washed with water 3 times followed by brine, concentrated, and purified by column chromatography with 40% EtOAc/heptane to give **78** (1.32 g, 82%) as a red solid. LCMS [M+1] 394.0; $^1$H NMR (400 MHz, $CDCl_3$) δ ppm 7.83 (s, 1H), 7.10 (s, 1H), 4.75 (br. s., 2H), 4.69 (br. s., 1H), 3.87 (br. s., 2H), 3.75 (br. s., 1H), 3.66 (br. s., 1H), 1.46 - 1.51 (m, 9H). A mixture of **78** (760 mg, 1.93 mmol), 1-methyl-4-(tributylstannyl)-1H-imidazole **79** (1.43 g, 3.86 mmol) $Pd(PPh_3)_2Cl_2$ (136 mg, 0.193 mmol) in DMF (20 mL, 0.1 M) was microwaved at 120°C for 30 min. The reaction mixture was then diluted with water and EtOAc. The Pd was filtered and the aqueous was extracted with EtOAc 3 times. The organic layers were combined, concentrated and purified by column chromatography with 10% MeOH/EtOAc to afford **80** (690 mg, 90%) as brown oil which solidified upon vacuum. LCMS [M+1] 396.0. $^1$H NMR (400 MHz, $CDCl_3$) δ ppm 8.08 (br. s., 1H), 7.50 (br. s., 1H), 7.43 (br. s., 1H), 7.10 (br. s., 1H), 4.83 (br. s., 1H), 4.69 (br. s., 2H), 3.84 (br. s., 3H), 3.62 - 3.81 (m, 4H), 1.46 (s, 9H). *General TFA deprotection procedures G*. Compound **80** (700 mg, 1.77 mmol) was dissolved in 5 mL TFA, and stirred at room temperature for 1 hour. The solvent was evaporated and the residue was dried over vacuum to give 2.46 g brown oil which was used directly in the next coupling step. General HATU procedure **C** was used with **29**. The crude material was purified by chiral SFC to afford **18a** (317 mg, 35%) and **18b** (309 mg, 35%).

Compound **18a** - LCMS [M+1] 498.20; $^1$H NMR (400 MHz, DMSO-$d_6$) δ ppm 8.03 (s, 1H), 7.58 (s, 1H), 7.54 (br. s., 1H), 7.44 (s, 1H), 7.24 - 7.41 (m, 4H), 5.77 (d, J=10.88 Hz, 2H), 5.21 -5.40 (m, 1H), 4.18 - 4.46 (m, 1H), 3.99 - 4.18 (m, 1H), 3.87 - 3.99 (m, 1H), 3.73 - 3.86 (m, 3H), 3.60 - 3.69 (m, 3H); HRMS for $C_{22}H_{21}F_5N_5O_3$ MS m/z $[M+H]^+$ Calcd: 498.1559; found 498.1561.

Compound **18b** – LCMS [M+1] 498.20; $^1$H NMR (400 MHz, DMSO-$d_6$) δ ppm 8.03 (s, 1H) 7.58 (s, 1H) 7.54 (br. s., 1H) 7.44 (s, 1H) 7.24 - 7.41 (m, 4H) 5.77 (d, J=10.76 Hz, 2H) 5.21 - 5.38 (m, 1H) 4.17 - 4.46 (m, 1H) 3.98 - 4.17 (m, 1H) 3.87 - 3.98 (m, 1H) 3.69 - 3.86 (m, 3H) 3.67 (d, J=1.71 Hz, 3H); HRMS for $C_{22}H_{21}F_5N_5O_3$ MS m/z $[M+H]^+$ Calcd: 498.1559; found 498.1562.

**(S)-6-amino-5-((4,4-difluoro-1-(2-(4-(trifluoromethoxy)phenyl)acetyl)pyrrolidin-3-yl)oxy)-N-methylnicotinamide (19).** Compound **78** (500 mg, 1.27 mmol) was dissolved in MeOH (35 mL, 0.036 M), $Pd(OAc)_2$ (23 mg, 0.10 mmol), $Et_3N$ (575 mg, 5.68 mmol), DPPF (47 mg, 0.085 mmol) and DMF (575 mg, 7.8 mmol) were added. The reaction mixture was heated at 80°C overnight under 5.2 bar CO, and then cooled to room temperature, filtered and concentrated. The product was purified by column chromatography with 50% EtOAc/heptane to afford **81** (307 mg, 65% yield) an off white solid. LCMS [M+1] 374.0; $^1$H NMR (400 MHz, $CDCl_3$) δ ppm 8.44 (s, 1H), 7.55 (s, 1H), 5.38 (br. s., 2H), 4.82 (br. s., 1H), 3.82 - 3.97 (m, 6H), 3.78 (br. s., 1H), 1.49 (s, 9H). General TFA procedures **G** and HATU coupling procedures **C** were used to afford **82** (370 mg, 95%). LCMS [M+1] 475.90; $^1$H NMR (400 MHz, DMSO-$d_6$) δ ppm 8.23 - 8.29 (m, 1H) 7.57 (dd, J=10.51, 1.47 Hz, 1H) 7.25 - 7.40 (m, 4H) 6.86 (br. s., 2H) 5.32 -5.48 (m, 1H) 4.17 - 4.46 (m, 1H) 3.99 - 4.17 (m, 2H) 3.88 - 3.99 (m, 1H) 3.79 (d, J=1.47 Hz, 3H) 3.64 - 3.77 (m, 2H) 3.18 (d, J=5.26 Hz, 2H). Compound **82** (370 mg, 0.778 mmol) was dissolved in MeOH (5 mL, 0.2 M), and NaOH (2.0 N, 156 mg, 1.94 mL, 3.89 mmol) was added. The reaction mixture was heated at 60°C for 1 hour. MeOH was evaporated and the mixture was acidified by conc. HCl. The material was lyophilized to afford (614 mg, >100% yield) as a white solid which was used without further purification. LCMS [M+1] 461.85. General HATU coupling procedure **C** was used with methyl amine followed by standard chiral separation to obtain **19** (76 mg, 41%); LCMS [M+1] 475.20; $^1$H NMR (400 MHz, DMSO-$d_6$) δ ppm 8.16 (s, 1H) 8.05 - 8.14 (m, 1H) 7.58 (br.

s., 1H) 7.24 - 7.43 (m, 4H) 6.43 (br. s., 1H) 6.40 (br. s., 1H) 5.18 - 5.35 (m, 1H) 4.17 - 4.46 (m, 1H) 4.08 - 4.17 (m, 1H) 3.85 - 3.99 (m, 1H) 3.63 - 3.85 (m, 3H) 2.69 - 2.83 (m, 3H);. HRMS for $C_{20}H_{20}F_5N_4O_4$ MS m/z $[M+H]^+$ Calcd: 475.1399, Found: 475.1404.

**(S)-6-amino-5-((4,4-difluoro-1-(2-(4-(trifluoromethoxy)phenyl)acetyl)pyrrolidin-3-yl)oxy)-N-ethylnicotinamide (20).** See procedures for **19** and general HATU coupling procedure **C** with ethyl amine, followed by standard chiral separation (20 mg, 25%); LCMS [M+1] 489.00; $^1$H NMR (400 MHz, DMSO-$d_6$) δ ppm 8.11 - 8.21 (m, 2H), 7.59 (d, J=2.08 Hz, 1H), 7.25 - 7.41 (m, 4H), 6.41 (s, 1H), 6.44 (s, 1H), 5.19 - 5.37 (m, 1H), 4.17 - 4.47 (m, 1H), 4.00 - 4.17 (m, 1H), 3.87 - 4.00 (m, 1H), 3.65 - 3.84 (m, 3H), 3.22 - 3.29 (m, 2H), 1.12 (td, J=7.21, 1.47 Hz, 3H).

**Computational modelling methods.** All molecules were prepared for docking simulation using LigPrep 2.5 (Schrödinger) to consider proper protonation states and tautomers. The docking simulation was performed with Glide 5.8 (Schrödinger) using protein models based on in-house X-ray structures. Docking poses were minimized using the OPLS2005 force field.

**Metabolism of compounds in human liver microsomes (HLM) in vitro.** Stability of compounds in human liver microsomes (HLM) in vitro was determined at a compound concentration of 1μM. Incubations (32.5μL) contained HLM (Pfizer Global supply) at a protein concentration of 0.71mg/mL and were supplemented with a reducing equivalent regenerating system (isocitrate/isocitrate dehydrogenase). The assay cocktail was incubated at 37ºC for up to 60 min in the presence and absence of $NADP^+$ (2 mM) and samples withdrawn at time intervals and reactions terminated by addition to 75μL of acetonitrile and 65μL of water. Samples were centrifuged to remove precipitated protein and the supernatants dried under a stream of nitrogen. Dried extracts were reconstituted in 100μL of 50/50 acetonitrile/water + 0.1% formic acid and further diluted with 100μL of 5/95 acetonitrile/water containing 0.1% formic acid. Following further

centrifugation, samples (5μL) were analyzed by LC-MS/MS using a QTOF Premier (s/n: HAA053) mass spectrometer (Waters) operated in positive ion mode and data were acquired in the multiple reaction monitoring (MRM) mode using argon as the collision gas. The natural log of ratios of peak areas of test compound to a reference internal standard were plotted against incubation time and apparent intrinsic clearance ($CL_{int}$) calculated form the slope of the line.

**Metabolism of compounds in human hepatocytes (hHep) in vitro.** Stability of compounds in human hepatocytes (hHEP) (Bioreclamation Inc., NY, USA) in vitro was determined at a compound concentration of 1μM. Incubations (22.5μL) in Williams E medium containing 0.75 x $10^6$ cells/mL were carried out at 37ºC in an atmosphere of 95/5 air:$CO_2$ at 95% humidity for up to 240 min. Incubations were terminated with 50μL cold acetonitrile and samples were centrifuged to remove precipitated protein. Samples of 35μL of supernatant were diluted with 120μL water prior to analysis of compound by LC-MS/MS according to the method described for microsomal incubations. $CL_{int}$ was calculated as described for HLM, above.

**Determination of permeability in RRCK cell monolayers.** Apparent permeability ($P_{app}$) was determined in the apical to basolateral (A/B) direction in monolayers of low transporter expressing MDCK cells (RRCK) according to published methods.[35]

**Determination of efflux by P-gp and BCRP.** Apparent permeability ($P_{app}$) was determined in apical to basolateral (A/B) and basolateral to apical (B/A) directions in monolayers of MDCK cells transfected with either human MDR1 of human BCRP according to published methods.[51] Efflux ratio (ER) was used as an index of efflux, whereby ER= $P_{app}$ B/A / $P_{app}$ A/B.

AUTHOR INFORMATION

**Corresponding Author**

*Email: sharan.bagal@outlook.com

**Notes**

The authors declare no competing financial interest.

**ACKNOWLEDGMENT**

The authors would like to thank Dr. Katrina Gore for statistical analysis of UVIH data, Dr. Beth Lunney, Dr. Alan Brown, Dr. Martin Wythes, Dr. Nigel Swain and Dr. Martin Edwards for useful discussions and Neal Sach for synthesis and TCG Lifesciences for synthesis and screening.

**ABBREVIATIONS**

AB, apical to basolateral; AO, aldehyde oxidase; ATP, adenosine triphosphate; BA, basolateral to apical; $B_2Pin_2$, Bis(pinacolato)diboron; Boc, tert-butyloxycarbonyl; BCRP, breast cancer resistance protein; BDNF, brain derived neurotrophic factor; BBB, blood-brain barrier; $C_{b,u}/C_{p,u}$, unbound brain/plasma concentration ratio; ID, compound identification number; $C_{avg}$, average plasma concentration; CNS, central nervous system; CYP, cytochrome P450; DIBAL-H, diisobutylaluminium hydride; ER, efflux ratio; F, oral bioavailability; hERG, human ether-a-go-go related gene; hHep, human hepatocytes; HLM, human liver microsomes; $IC_{50}$, half-maximum inhibitory concentration; $K_a$, association rate; $K_d$, dissociation rate; $K_D$, dissociation constant; LE, ligand efficiency; LipE, lipophilic efficiency; LogD, distribution coefficient at pH 7.4; MDCK, Madine Darby canine kidney; MDR1, multidrug resistance protein (*p*-glycoprotein); MW,

molecular weight; ND, not determined; NT3, neurotrophin 3; NT4, neurotrophin 4; NGF, nerve growth factor; $P_{app}$, apparent permeability; PDB, Protein Data Bank; P-gp, p-glycoprotein; PK, pharmacokinetics; PSA, polar surface area; RRCK, Ralph Russ canine kidney cell line, permeability measured with low-efflux MDCK cell line; SBDD, structure based drug design; $T_{1/2}$, half-life; TI, therapeutic index; Trk, tropomyosin related kinase; UVIH, ultraviolet burn induced hyperalgesia; $V_{ss}$, volume of distribution at steady state.

## ASSOCIATED CONTENT

**Supporting Information**. The Supporting Information is available free of charge on the ACS publications website. Molecular formula strings are provided along with Surface plasmon resonance data for ligands **10b**, **13b** and **19**, Trk cell based assay protocols, Metabolite identification data for compounds **10b**, **13b** and **19**, Kinase selectivity data for compounds **10b, 13b** and **19**, Ultraviolet irradiation-induced thermal hyperalgesia data in rats for **10b**, **13b** and **19**, Measurement of CNS penetration in rats, Solubility determination method, Chemical abbreviations, General experimental conditions, Commercial starting materials, NMR and LCMS spectra of **10b**, **13b**, and **19**.

## Accession Codes

PDB codes are 6DKW for compound **3**, 6DKB for compound **10b**, 6DKG for compound **13b** and 6DKI for compound **19**. Authors will release the atomic coordinates and experimental data upon article publication.

## REFERENCES

1. Skaper, S. D. The Neurotrophin Family of Neurotrophic Factors: An Overview. *Methods Mol. Biol.* **2012,** *846* (Neurotrophic Factors), 1-12.

2. Hefti, F. F.; Rosenthal, A.; Walicke, P. A.; Wyatt, S.; Vergara, G.; Shelton, D. L. Davies, A. M. Novel Class of Pain Drugs Based on Antagonism of NGF. *Trends Pharmacol. Sci.* **2006,** *27* (2), 85-91.

3. Lane, N. E.; Schnitzer, T. J.; Birbara, C. A.; Mokhtarani, M.; Shelton, D. L.; Smith, M. D. Brown, M. T. Tanezumab for the Treatment of Pain from Osteoarthritis of the Knee. *N. Engl. J. Med.* **2010,** *363* (16), 1521.

4. Schnitzer, T. J.; Lane, N. E.; Birbara, C.; Smith, M. D.; Simpson, S. L. Brown, M. T. Long-Term Open-Label Study of Tanezumab for Moderate to Severe Osteoarthritic Knee Pain. *Osteoarthritis Cartilage* **2011,** *19* (6), 639-646.

5. Evans, R. J.; Moldwin, R. M.; Cossons, N.; Darekar, A.; Mills, I. W. Scholfield, D. Proof of Concept Trial of Tanezumab for the Treatment of Symptoms Associated with Interstitial Cystitis. *J. Urol. (N. Y., NY, U. S.)* **2011,** *185* (5), 1716-1721.

6. Katz, N.; Borenstein, D. G.; Birbara, C.; Bramson, C.; Nemeth, M. A.; Smith, M. D. Brown, M. T. Efficacy and Safety of Tanezumab in the Treatment of Chronic Low Back Pain. *Pain* **2011,** *152* (10), 2248-2258.

7. Gavrin, L. K. Saiah, E. Approaches to Discover Non-ATP Site Kinase Inhibitors. *MedChemComm* **2013,** *4* (1), 41-51.

8. Capdeville, R.; Buchdunger, E.; Zimmermann, J. Matter, A. Glivec (STI571, Imatinib), a Rationally Developed, Targeted Anticancer Drug. *Nat Rev Drug Discov* **2002,** *1* (7), 493-502.

9. Skerratt, S. E.; Andrews, M.; Bagal, S. K.; Bilsland, J.; Brown, D.; Bungay, P. J.; Cole, S.; Gibson, K. R.; Jones, R.; Morao, I.; Nedderman, A.; Omoto, K.; Robinson, C.; Ryckmans, T.; Skinner, K.; Stupple, P. Waldron, G. The Discovery of a Potent, Selective, and Peripherally Restricted Pan-Trk Inhibitor (PF-06273340) for the Treatment of Pain. *Journal of Medicinal Chemistry* **2016,** *59* (22), 10084-10099.

10. Mueller, M. In Vivo Function of NGF/TrkA Signaling in the Cholinergic Neurons of the Murine Basal Forebrain. Ph.D Dissertation, Ludwig-Maximilians-University, Munich, 2005.

11. Mufson, E. J. Kordower, J. H. In *Nerve Growth Factor Systems in Alzheimer's Disease*, Kluwer Academic/Plenum Publishers: 1999; pp 681-731.

12. Sanchez-Ortiz, E.; Yui, D.; Song, D.; Li, Y.; Rubenstein, J. L.; Reichardt, L. F. Parada, L. F. TrkA Gene Ablation in Basal Forebrain Results in Dysfunction of the Cholinergic Circuitry. *J. Neurosci.* **2012,** *32* (12), 4065-4079.

13. Mattson, M. P. Glutamate and Neurotrophic Factors in Neuronal Plasticity and Disease. *Ann. N. Y. Acad. Sci.* **2008,** *1144* (Neural Signaling Opportunities for Novel Diagnostic Approaches and Therapies), 97-112.

14. Minichiello, L. TrkB Signalling Pathways in LTP and Learning. *Nat Rev Neurosci* **2009,** *10* (12), 850-860.

15. Mason, B. L.; Lobo, M. K.; Parada, L. F. Lutter, M. Trk B Signaling in Dopamine 1 Receptor Neurons Regulates Food Intake and Body Weight. *Obesity* **2013,** *21* (11), 2372-2376.

16. Noble, E. E.; Billington, C. J.; Kotz, C. M. Wang, C. The Lighter Side of BDNF. *Am. J. Physiol.* **2011,** *300* (5, Pt. 2), R1053-R1069.

17. Yeo, G. S. H.; Connie Hung, C.-C.; Rochford, J.; Keogh, J.; Gray, J.; Sivaramakrishnan, S.; O'Rahilly, S. Farooqi, I. S. A De Novo Mutation Affecting Human TrkB Associated with Severe Obesity and Developmental Delay. *Nat Neurosci* **2004,** *7* (11), 1187-1189.

18. Lindholm, D.; Castrén, E.; Tsoulfas, P.; Kolbeck, R.; Berzaghi, M. d. P.; Leingärtner, A.; Heisenberg, C.; Tessarollo, L.; Parada, L.; Thoenen, H. Tesarollo, L. Neurotrophin-3 Induced by Tri-Iodothyronine in Cerebellar Granule Cells Promotes Purkinje Cell Differentiation. *The Journal of Cell Biology* **1993,** *122* (2), 443-450.

19. Zhou, X.-F. Rush, R. A. Functional Roles of Neurotrophin 3 in the Developing and Mature Sympathetic Nervous System. *Molecular Neurobiology 13* (3), 185-197.

20. Wang, T.; Yu, D. Lamb, M. L. Trk Kinase Inhibitors as New Treatments for Cancer and Pain. *Expert Opin. Ther. Pat.* **2009,** *19* (3), 305-319.

21. Bagal, S. Bungay, P. Restricting Cns Penetration of Drugs to Minimise Adverse Events: Role of Drug Transporters. *Drug Discov Today Technol* **2014,** *12*, e79-85.

22. Cole, S.; Bagal, S.; El-Kattan, A.; Fenner, K.; Hay, T.; Kempshall, S.; Lunn, G.; Varma, M.; Stupple, P. Speed, W. Full Efficacy with No CNS Side-Effects: Unachievable Panacea or Reality?? DMPK Considerations in Design of Drugs with Limited Brain Penetration. *Xenobiotica* **2012,** *42* (1), 11-27.

23. Wager, T. T.; Liras, J. L.; Mente, S. Trapa, P. Strategies to Minimize Cns Toxicity: In Vitro High-Throughput Assays and Computational Modeling. *Expert Opin. Drug Metab. Toxicol.* **2012,** *8* (5), 531-542.

24. Kalvass, J. C.; Polli, J. W.; Bourdet, D. L.; Feng, B.; Huang, S. M.; Liu, X.; Smith, Q. R.; Zhang, L. K. Zamek-Gliszczynski, M. J. Why Clinical Modulation of Efflux Transport at the

Human Blood-Brain Barrier Is Unlikely: The ITC Evidence-Based Position. *Clin. Pharmacol. Ther.* **2013,** *94* (1), 80-94.

25. Giacomini, K. M.; Huang, S.-M.; Tweedie, D. J.; Benet, L. Z.; Brouwer, K. L. R.; Chu, X.; Dahlin, A.; Evers, R.; Fischer, V.; Hillgren, K. M.; Hoffmaster, K. A.; Ishikawa, T.; Keppler, D.; Kim, R. B.; Lee, C. A.; Niemi, M.; Polli, J. W.; Sugiyama, Y.; Swaan, P. W.; Ware, J. A.; Wright, S. H.; Wah Yee, S.; Zamek-Gliszczynski, M. J. Zhang, L. Membrane Transporters in Drug Development. *Nat. Rev. Drug Discovery* **2010,** *9* (3), 215-236.

26. Leeson, P. D. Springthorpe, B. The Influence of Drug-Like Concepts on Decision-Making in Medicinal Chemistry. *Nat. Rev. Drug Discovery* **2007,** *6* (11), 881-890.

27. Bagal, S. K. Bungay, P. J. Minimizing Drug Exposure in the CNS While Maintaining Good Oral Absorption. *ACS Medicinal Chemistry Letters* **2012,** *3* (12), 948-950.

28. Tachibana, T.; Kato, M. Sugiyama, Y. Prediction of Nonlinear Intestinal Absorption of Cyp3a4 and P-Glycoprotein Substrates from Their in Vitro Km Values. *Pharm. Res.* **2012,** *29* (3), 651-668.

29. Andrews, M. D.; Bagal, S. K.; Gibson, K. R.; Omoto, K.; Ryckmans, T.; Skerratt, S. E. Stupple, P. A. Pyrrolo[2,3-D]Pyrimidine Derivatives as Inhibitors of Tropomyosin-Related Kinases and Their Preparation and Use in the Treatment of Pain. WO2012137089A1, 2012.

30. Loudon, P.; Siebenga, P.; Gorman, D.; Gore, K.; Dua, P.; van Amerongen, G.; Hay, J. L.; Groeneveld, G. J. Butt, R. P. Demonstration of an Anti-Hyperalgesic Effect of a Novel Pan-Trk Inhibitor PF-06273340 in a Battery of Human Evoked Pain Models. *Br. J. Clin. Pharmacol.* **2018,** *84* (2), 301-309.

31. Skerratt, S. E.; Bagal, S. K.; Swain, N. A.; Omoto, K. Andrews, M. D. Preparation of N-Acylpiperidine Ethers as Tropomyosin-Related Kinase Inhibitors. WO2015092610A1, 2015.

32. Deacon, M.; Singleton, D.; Szalkai, N.; Pasieczny, R.; Peacock, C.; Price, D.; Boyd, J.; Boyd, H.; Steidl-Nichols, J. V. Williams, C. Early Evaluation of Compound Qt Prolongation Effects: A Predictive 384-Well Fluorescence Polarization Binding Assay for Measuring Herg Blockade. *Journal of Pharmacological and Toxicological Methods* **2007,** *55* (3), 255-264.

33. Jamieson, C.; Moir, E. M.; Rankovic, Z. Wishart, G. Medicinal Chemistry of Herg Optimizations: Highlights and Hang-Ups. *Journal of Medicinal Chemistry* **2006,** *49* (17), 5029-5046.

34. Varma, M. V.; Gardner, I.; Steyn, S. J.; Nkansah, P.; Rotter, C. J.; Whitney-Pickett, C.; Zhang, H.; Di, L.; Cram, M.; Fenner, K. S. El-Kattan, A. F. pH-Dependent Solubility and Permeability Criteria for Provisional Biopharmaceutics Classification (BCS and BDDCS) in Early Drug Discovery. *Molecular Pharmaceutics* **2012,** *9* (5), 1199-1212.

35. Di, L.; Whitney-Pickett, C.; Umland, J. P.; Zhang, H.; Zhang, X.; Gebhard, D. F.; Lai, Y.; Federico, J. J.; Davidson, R. E.; Smith, R.; Reyner, E. L.; Lee, C.; Feng, B.; Rotter, C.; Varma, M. V.; Kempshall, S.; Fenner, K.; El-kattan, A. F.; Liston, T. E. Troutman, M. D. Development of a New Permeability Assay Using Low-Efflux MDCKII Cells. *J. Pharm. Sci.* **2011,** *100*, 4974-4985.

36. Bagal, S. K.; Omoto, K.; Skerratt, S. E.; Swain, N. A.; Cui, J. J. McAlpine, I. J. N-Acylpiperidine Ether Tropomyosin-Related Kinase Inhibitors. WO2016009296A1, 2016.

37. Miao, Z. Scott Obach, R., Chapter 10 Alcohols and Phenols: Absorption, Distribution, Metabolism and Excretion. In *Metabolism, Pharmacokinetics and Toxicity of Functional Groups: Impact of Chemical Building Blocks on ADMET*, Smith, D. A., Ed. The Royal Society of Chemistry: Cambridge UK, 2010; pp 460-485.

38. Xing, L.; Rai, B. Lunney, E. A. Scaffold Mining of Kinase Hinge Binders in Crystal Structure Database. *Journal of Computer-Aided Molecular Design* **2013,** *28* (1), 13-23.

39. Bagal, S. K.; Omoto, K.; Skerratt, S. E.; Cui, J. J.; Greasley, S. E.; McAlpine, I. J.; Nagata, A.; Ninkovic, S. Tran-Dube, M. B. Preparation of N-Acylpyrrolidine Ether Derivatives as TrkA Antagonists. WO2016020784, 2016.

40. Regan, J.; Pargellis, C. A.; Cirillo, P. F.; Gilmore, T.; Hickey, E. R.; Peet, G. W.; Proto, A.; Swinamer, A. Moss, N. The Kinetics of Binding to P38 Map Kinase by Analogues of BIRB 796. *Bioorganic & Medicinal Chemistry Letters* **2003,** *13* (18), 3101-3104.

41. Di, L.; Trapa, P.; Obach, R. S.; Atkinson, K.; Bi, Y.-A.; Wolford, A. C.; Tan, B.; McDonald, T. S.; Lai, Y. Tremaine, L. M. A Novel Relay Method for Determining Low-Clearance Values. *Drug Metabolism and Disposition* **2012,** *40* (9), 1860-1865.

42. Yazdanian, M., Overview of Determination of Biopharmaceutical Properties for Development Candidate Selection. In *Current Protocols in Pharmacology*, John Wiley & Sons, Inc.: 2001.

43. Lovering, F.; Bikker, J. Humblet, C. Escape from Flatland: Increasing Saturation as an Approach to Improving Clinical Success. *Journal of Medicinal Chemistry* **2009,** *52* (21), 6752-6756.

44. Yalkowsky, S. H. Valvani, S. C. Solubility and Partitioning I: Solubility of Nonelectrolytes in Water. *Journal of Pharmaceutical Sciences* **1980,** *69* (8), 912-922.

45. Wan, S.; Bhati, A. P.; Skerratt, S.; Omoto, K.; Shanmugasundaram, V.; Bagal, S. K. Coveney, P. V. Evaluation and Characterization of Trk Kinase Inhibitors for the Treatment of Pain: Reliable Binding Affinity Predictions from Theory and Computation. *Journal of Chemical Information and Modeling* **2017,** *57* (4), 897-909.

46. Wang, L.; Berne, B. J. Friesner, R. A. On Achieving High Accuracy and Reliability in the Calculation of Relative Protein–Ligand Binding Affinities. *Proceedings of the National Academy of Sciences* **2012,** *109* (6), 1937-1942.

47. Wang, L.; Friesner, R. A. Berne, B. J. Replica Exchange with Solute Scaling: A More Efficient Version of Replica Exchange with Solute Tempering (REST2). *The Journal of Physical Chemistry B* **2011,** *115* (30), 9431-9438.

48. Darout, E.; Guimaraes, C.; Mascitti, V. McClure, K. F. Preparation of Pyridinyl Pyrimidinyl Piperidine Compounds as GPR119 Modulators for Therapy. WO2013011402A1, 2013.

49. Cui, J. J.; Funk, L. A.; Jia, L.; Kung, P.-P.; Meng, J. J.; Nambu, M. D.; Pairish, M. A.; Shen, H. Tran-Dube, M. B. Preparation of Aminoheteroaryl Compounds as C-Met Tyrosine Kinase Inhibitors. WO2006021886A1, 2006.

50. Johnson, T. W.; Richardson, P. F.; Collins, M. R.; Richter, D. T.; Burke, B. J.; Gajiwala, K.; Ninkovic, S.; Linton, M. A.; Le, P. T. Q. Hoffman, J. E. Preparation of Pyrimidine Derivatives and Triazoles as Axl Inhibitors. WO2016097918 2016.

51. Zhou, L.; Schmidt, K.; Nelson, F. R.; Zelesky, V.; Troutman, M. D. Feng, B. The Effect of Breast Cancer Resistance Protein and P-Glycoprotein on the Brain Penetration of Flavopiridol, Imatinib Mesylate (Gleevec), Prazosin, and 2-Methoxy-3-(4-(2-(5-Methyl-2-Phenyloxazol-4-Yl)Ethoxy)Phenyl)Propanoic Acid (PF-407288) in Mice. *Drug Metab. Dispos.* **2009,** *37*, 946-955.

## Table of Contents Graphic